HHS Public Access

Author manuscript

J Comp Neurol. Author manuscript; available in PMC 2021 June 01.

Published in final edited form as:

J Comp Neurol. 2020 June ; 528(8): 1436–1456. doi:10.1002/cne.24834.

Structural Plasticity of GABAergic and Glutamatergic Networks in the Motor Thalamus of Parkinsonian Monkeys

Ashley J. Swain[1,2], **Adriana Galvan**[1,2,3], **Thomas Wichmann**[1,2,3], **Yoland Smith**[1,2,3]

[1]Division of Neuropharmacology and Neurological Disorders, Yerkes National Primate Research Center, Emory University, Atlanta, Georgia, USA

[2]Udall Center of Excellence for Parkinson's Disease Research, Emory University, Atlanta, Georgia, USA

[3]Department of Neurology, School of Medicine, Emory University, Atlanta, Georgia, USA

Abstract

In the primate thalamus, the parvocellular ventral anterior nucleus (VApc) and the centromedian nucleus (CM) receive GABAergic projections from the internal globus pallidus (GPi) and glutamatergic inputs from motor cortices. In this study, we used electron microscopy to assess potential structural changes in GABAergic and glutamatergic microcircuits in the VApc and CM of MPTP-treated parkinsonian monkeys.

The intensity of immunostaining for GABAergic markers in VApc and CM did not differ between control and parkinsonian monkeys. In the electron microscope, three major types of terminals were identified in both nuclei: (1) vesicular glutamate transporter 1 (vGluT1)-positive terminals forming asymmetric synapses (type As), which originate from the cerebral cortex, (2) GABAergic terminals forming single symmetric synapses (type S1), which likely arise from the reticular nucleus and GABAergic interneurons, and (3) GABAergic terminals forming multiple symmetric synapses (type S2), which originate from GPi. The density of As terminals outnumbered that of S1 and S2 terminals in VApc and CM of control and parkinsonian animals. No significant change was found in the abundance and synaptic connectivity of S1 and S2 terminals in VApc or CM of MPTP-treated monkeys, while the prevalence of "As" terminals in VApc of parkinsonian monkeys was 51.4% lower than in controls. The cross-sectional area of vGluT1-positive boutons in both VApc and CM of parkinsonian monkeys was significantly larger than in controls, but their pattern of innervation of thalamic cells was not altered. Our findings suggest that the corticothalamic system undergoes significant synaptic remodeling in the parkinsonian state.

Graphical Abstract

Reduced prevalence and increased size of glutamatergic cortical terminals in contact with thalamocortical neurons in the basal ganglia-receiving region of the ventral motor thalamus in MPTP-treated parkinsonian monkeys. The electron micrographs show vGluT1-immunoreactive

Corresponding Author: Yoland Smith, PhD, ysmit01@emory.edu, *Phone*: (404) 727 7519, *Address*: 954 Gatewood Road NE, Atlanta, GA 30329, USA.

Data availability statement: The data that support the findings of this study are available from the corresponding author upon reasonable request

corticothalamic terminals in normal and parkinsonian monkeys. Abbreviations: CTv, CTvi: Corticothalamic neurons, layer 5, layer 6; Den: Dendrite; Glut: Glutamatergic terminal; GPi: Globus pallidus, internal segment; IN: GABAergic interneuron; RTN: Reticular nucleus; TC: Thalamocortical neuron.

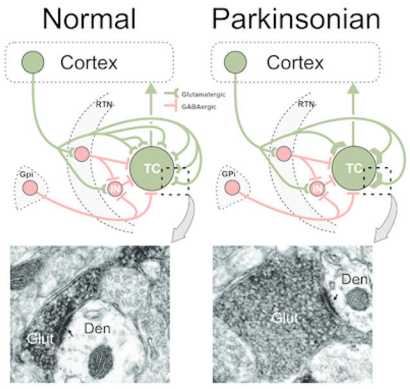

Keywords

Pallidothalamic; corticothalamic; primate; centromedian nucleus; ventral anterior nucleus; parkinsonism; RRDIs: AB_2814814; AB_2278725; AB_2254256; AB_221569; AB_2814813; AB_477652; AB_2201528

INTRODUCTION

In the primate thalamus, the parvocellular part of the ventral anterior nucleus (VApc) and the centromedian nucleus (CM) are the main targets of inhibitory (GABAergic) inputs from the internal pallidal segment (GPi), the primary motor output nucleus of the basal ganglia (Parent et al., 1983; Parent et al., 2001; Parent and Parent, 2004). The VApc is the main source of thalamic inputs to the supplementary motor area and premotor cortex, while the CM gives rise to a massive innervation of the sensorimotor striatum (Akkal et al., 2007; Inase et al., 1996; McFarland and Haber, 2000; McFarland and Haber, 2001; Sadikot et al., 1992; Sakai et al., 1999; Sakai et al., 2000; Schell and Strick, 1984; Shindo et al., 1995; Sidibé and Smith, 1996; Smith and Parent, 1986; Smith et al., 2014; Tokuno et al., 1992). In addition to massive GABAergic inputs from the GPi, the VApc and CM receive prominent glutamatergic inputs from the cerebral cortex and GABAergic afferents from the reticular thalamic nucleus and GABAergic interneurons, which in primates (but not in rodents), account for 15-30% of the total neuronal population of VApc and CM ((Ilinsky and Kultas-Ilinsky, 1990; Jones, 2007; Smith et al., 1987). Despite their high prevalence in the primate thalamus, the anatomy and synaptic integration of GABAergic interneurons in the microcircuitry of the motor thalamus is largely unknown.

In traditional models of the pathophysiology of Parkinson’s disease (PD), the loss of nigrostriatal dopamine (DA) increases the activity of the inhibitory basal ganglia output projections to the ventral motor thalamus, leading to reduced activity of thalamocortical projections (Albin et al., 1989; DeLong, 1990). Recent studies have identified altered

activity (including firing rate changes, bursting, oscillatory firing properties, and altered somatosensory responses) of thalamic cells in the VApc of animal models of PD and in PD patients (Aymerich et al., 2006; Bosch-Bouju et al., 2014; Chen et al., 2010; Guehl et al., 2003; Hirsch et al., 2000; Kammermeier et al., 2016; Lanciego et al., 2009; Magnin et al., 2000; Mitchell et al., 1989; Molnar et al., 2005; Ni et al., 2000; Orieux et al., 2000; Pessiglione et al., 2005; Raeva et al., 1999; Rolland et al., 2007; Sarnthein and Jeanmonod, 2007; Schneider and Rothblat, 1996; Zirh et al., 1998).

In the basal ganglia, the parkinsonian state is associated with characteristic morphologic and ultrastructural changes. Thus, in the striatum and subthalamic nucleus (STN), the dopamine-depleted state is accompanied by substantial remodeling of specific synaptic microcircuits. In particular, significant changes in the number and ultrastructural features of cortical terminals, associated with robust alterations in electrophysiological and plastic properties of corticostriatal and corticosubthalamic synapses have been reported in rodent and primate models of PD (Chu et al., 2017; Day et al., 2006; Deutch, 2006; Ingham et al., 1998; Mathai and Smith, 2011; Mathai et al., 2015; Raju et al., 2008; Villalba et al., 2009; Villalba and Smith, 2010; Villalba and Smith, 2011; Villalba et al., 2015). In the STN of dopamine-depleted mice, there is a significant increase in the number of synapses formed by individual GABAergic terminals from the external segment of the globus pallidus (GPe), accompanied with increased synaptic strength of pallidosubthalamic synapses (Chu et al., 2017; Fan et al., 2012).

The possibility that similar structural alterations also occur in glutamatergic and GABAergic thalamic microcircuits in the parkinsonian state has not been examined. The objective of the present study was to compare the relative prevalence, pattern of synaptic connectivity and ultrastructural features of glutamatergic and GABAergic inputs to thalamocortical neurons and interneurons in the VApc and CM in control and MPTP-treated parkinsonian monkeys. Having such knowledge is critical to a deeper understanding of changes in thalamocortical and corticothalamic interactions in PD.

MATERIALS AND METHODS

Animals

Twenty-two rhesus macaque monkeys (*Macaca mulatta*) (12 males, 10 females; 2.5-17 years old; Table 1) obtained from the Yerkes National Primate Research Center colony) were used in these studies. All animals were housed in temperature-controlled rooms and exposed to a 12-hour light cycle. The animals were fed twice daily with monkey chow supplemented with fruits and vegetables and received ad lib water. All animal procedures were approved by the Institutional Animal Care and Use Committee (IACUC) of Emory University, and were performed according to the Guide for the Care and Use of Laboratory Animals and the U.S. Public Health Service Policy on the Humane Care and Use of Laboratory Animals. See Table 1 for more details on animals.

MPTP treatment and assessment of parkinsonism

Ten animals were rendered parkinsonian in the course of these studies. These animals received weekly MPTP injections (0.2-0.8 mg/kg i.m.; cumulative doses: 2.8–26.79 mg/kg; Natland International, Morrisville, NC or Sigma, St. Louis, MO), until they reached comparable states of stable, moderate parkinsonism. As described in previous studies (Bogenpohl et al., 2012; Devergnas et al., 2014; Galvan et al., 2010; Kliem et al., 2009; Masilamoni et al., 2010; Masilamoni et al., 2011; Wichmann et al., 2001; Wichmann and Soares, 2006), we assessed the severity of parkinsonism weekly for 15-min periods in an observation cage that was equipped with infrared beams, allowing us to measure their body movements as infrared beam break events. In addition, we used a parkinsonism rating scale to quantify impairments in 10 aspects of motor function (speed of movement, incidence and severity of “freezing” episodes, extremity posture, trunk posture, presence and severity of tremor, amount of arm movements, amount of leg movements, finger dexterity, home cage activity, and balance). Each item was scored on a 0–3 scale (maximal score, 30). The final parkinsonian motor scores ranged between 4.5-16, corresponding to mild and moderately severe parkinsonism. The severity of the parkinsonian motor signs had to be stable for a period of at least 6 weeks after the last MPTP injection before the monkeys were considered parkinsonian for this study. We have used the same protocol in many previous studies (Bogenpohl et al., 2013; Devergnas et al., 2016; Galvan et al., 2014; Hadipour-Niktarash et al., 2012; Masilamoni et al., 2010; Masilamoni et al., 2011; Masilamoni and Smith, 2017; Mathai et al., 2015; Villalba et al., 2014).

Anterograde labeling of pallidothalamic terminals

In 2 control and 2 MPTP-treated monkeys, pallidothalamic terminals were labeled anterogradely with viral vector injections in the GPi. A total of 2-8 μl of AAV5-hSyn-ChR2-EYFP or AAV5-hSyn-Arch3-EYFP was delivered in the GPi. In the control monkeys, the injections were made under isoflurane anesthesia with the animal fixed in a stereotaxic frame using aseptic surgical procedures. Pre-operative MRI scans of these monkeys were performed to help define the stereotaxic coordinates. Small holes were drilled in the skull and a Hamilton microsyringe was used to inject the viral vector at a single site in the ventrolateral part of GPi. To deliver the viral vector solution, the plunger of the syringe was pressed manually at an approximate rate of 1 μl/5 min. After completion, the syringe was left in place for 10 min before withdrawing. At the end of the surgery, the skin was sutured and the animals were treated with analgesics. The animals were allowed to survive for at least six months after injection.

In the MPTP-treated monkeys, the viral vector solutions were delivered in the GPi using extracellular recordings as a guide to delineate the borders of the neighboring nuclei using procedures previously described from our laboratory (Galvan et al., 2010; Kliem et al., 2007). Preparatory to the injections, recording chambers were stereotactically directed at the pallidum on either side of the brain, placed at an angle of 40° from the vertical in the coronal plane. The chambers were then affixed to the skull with dental acrylic, along with metal holders for head stabilization. Metal screws were used to anchor the acrylic to the bone.

During sessions conducted 2 to 3 weeks' post-surgery, electrophysiological mapping served to outline the borders of GPe and GPi. GPi cells were identified based on the depth of the electrode (at least 2 mm ventral to the first GPe unit), the presence of 'border' cells between GPe and GPi (DeLong, 1971), and the presence of neurons that fired at high frequency, characteristic for GPi cells (DeLong, 1971; Galvan et al., 2005; Galvan et al., 2011). The subsequent injections were done using a probe in which the injection tubing was combined with a recording microelectrode (Kliem and Wichmann, 2004). Extracellular recordings were conducted while lowering the injection system to help to define the final location of the injections in the GPi (Galvan et al., 2010; Kliem et al., 2007). A microsyringe connected to a pump was used to deliver the viral vector solutions at a rate of 0.1 to 0.2 μl/min. At the end of the injection, the injectrode was left in place for 10 min before withdrawing. These animals were allowed to survive for 1.5-7 months (during which the animals were used in other experiments)

All animals with virus injections were eventually perfusion-fixed as described below, and their brains prepared to allow immunohistochemical localization of the tag protein, enhanced yellow fluorescent protein (EYFP; see below).

Tissue collection

At the completion of the study, the animals were euthanized with pentobarbital, and transcardially perfused with a Ringer's solution and a mixture of paraformaldehyde (4%) and glutaraldehyde (0.1%). The brains were removed from the skull, post-fixed in 4% paraformaldehyde, and cut in serial sections (60 um) with a vibratome. The sections were stored at −20°C until further histological processing.

Immunohistochemistry

Tissue processing for microscopy.—Tissue processed for immunohistochemistry was prepared for light or electron microscopy (LM and EM, respectively). The tissue was pre-treated with 1% sodium borohydride in phosphate buffer solution for 20 min prior to immunohistochemistry processing. The sections were subsequently thoroughly washed in phosphate-buffered saline (PBS). Sections used for LM were incubated with antibodies as described below, while sections prepared for EM were placed in a cryoprotectant solution (phosphate buffer [PB], 0.05 M, pH 7.4, containing 25% sucrose and 10% glycerol) for 20 min, frozen at −80°C for 20 min, thawed, and returned to a graded series of cryoprotectant solution (100%, 70%, 50%, 30%) diluted in PBS. They were then washed in PBS before further processed.

The sections were pre-incubated in a solution containing 10% normal goat or horse serum (depending on the source of the primary antibody) and 1% bovine serum albumin (BSA) in PBS for 1 hour. For LM, 3% Triton-X-100 was used in addition to normal serum (NS) and BSA throughout the immunohistochemical reactions. Sections were then incubated with the respective primary antibodies for 48 hours at 4°C (for antibody dilutions and RRIDs, see Table 2) in a solution containing 1.0% NS and 1.0% BSA in PBS. Next, the sections were rinsed in PBS and transferred for 1.5 hours to a solution containing the secondary biotinylated antibody (dilution, 1:200). After rinsing with PBS, the sections were put in a

solution containing 1% avidin-biotin-peroxidase complex (Vector Laboratories, Burlingame, CA USA). The tissue was then washed in PBS and Tris buffer (0.05 M pH 7.6) before being transferred into a solution containing 0.01M imidazole, 0.005% hydrogen peroxide, and 0.025% 3,3′-diaminobenzidine tetrahydrochloride (DAB; Sigma, St. Louis, MO) in Tris for 10 min. The DAB reaction was terminated with several rinses of the sections in PBS. Sections prepared for LM were then mounted on gelatin-coated slides and prepared for observation.

Some sections were further processed for EM observations. These sections were transferred to PB (0.1 M, pH 7.4) for 10 min and exposed to 1% osmium tetroxide for 20 min. They were then rinsed with PB and dehydrated in an increasing gradient of ethanol. Uranyl acetate (1%) was added to the 70% alcohol step in the gradient to increase contrast. The sections were subsequently treated with propylene oxide before being embedded in epoxy resin (Durcupan, ACM; Fluka, Buchs, Switzerland) for 12 hours, mounted on microscope slides, and placed in a 60°C oven for 48 hours (Villalba and Smith, 2011). Blocks of tissue (1 mm^2) from the VApc and CM (2-4 blocks per animal) were then taken out from the slides and glued on top of resin blocks with cyanoacrylate glue. These blocks were trimmed and cut serially into 60-nm ultrathin serial sections with an ultramicrotome (Ultra-cut T2; Leica, Germany) and collected on single-slot Pioloform-coated copper grids. To limit our observations to tissue with similar antibody penetration, the EM analyses were restricted to ultrathin sections from the most superficial sections of blocks.

In control experiments, sections were processed as described above, but without primary antibodies (as a control for the specificity of binding of the secondary antibodies). The resulting sections were completely devoid of immunostaining following the incubations.

Striatal tyrosine hydroxylase (TH) immunostaining.—To verify denervation of the nigrostriatal pathway by MPTP intoxication, sections at the level of the striatum and the substantia nigra from MPTP-treated monkeys were stained with mouse anti-TH antibody (Table 2; RRID:AB_2201528), as described in our previous studies (Bogenpohl et al., 2013; Devergnas et al., 2016; Galvan et al., 2014; Hadipour-Niktarash et al., 2012; Masilamoni et al., 2010; Masilamoni et al., 2011; Masilamoni and Smith, 2017; Mathai et al., 2015).

Post-embedding GABA immunostaining.—To confirm the GABAergic phenotype of S1 and S2 terminals in VApc and CM, post-embedding immunogold labeling for GABA was carried out on thalamic tissue of one control and one MPTP-treated monkey, as described previously (Charara et al., 2005). Sections that were prepared for post-embedding EM immunolabeling underwent EM processing (osmium and tissue dehydration, as described above), were cut out and glued onto resin blocks, cut into ultrathin sections (60nm) and placed on gold slot grids. The sections were then incubated for 10 min on drops of Tris-buffered saline containing 0.01% Triton X-100 (TBS-T 0.01%; pH 7.6). Following pre-incubation, the grids were incubated overnight at room temperature with a well-characterized specific polyclonal GABA antiserum (Table 2; RRID:AB_477652), diluted in a solution of TBS-T 0.01%. After many washes in TBS-T (pH 7.6) and TBS (0.05M pH 8.2), the grids were then incubated for 90 min with 15 nm gold-conjugated secondary antibodies (1:50; Cedarlane Lab), diluted in TBS (pH 8.2). Grids were subsequently washed

in TBS (pH 8.2) and ultrapure water for 5 min. They were then incubated in a 2% aqueous solution of uranyl acetate for 90 min, and in distilled water for 5 min. The grids were subsequently stained with lead citrate.

vGAT and GAD67 immunoperoxidase labeling.—For LM analysis of changes in the intensity of immunostaining of markers for GABA terminals and cell bodies in the VApc and CM, every twelfth section (4-7 sections per animal) was stained for vGAT (Table 2; RRID:AB_2814814) or GAD67 (Table 2; RRID:AB_2278725) (Fig 1a and 1b). At the level of CM, adjacent sections were immunostained for calbindin (Cb) D28K (Table 2; RRID:AB_2254256) to help delineate the external border of the nucleus with the assistance of a rhesus monkey brain atlas (Lanciego and Vázquez, 2012).

GFP immunoperoxidase labeling.—In the 4 monkeys that received viral vector injections in the GPi (see above), the viral vector injection sites and the resulting anterograde labeling in the VApc and CM were localized using a specific GFP antibody (Table 2; AB_221569) and the immunoperoxidase ABC method. Note that this antibody also labels EYFP, the tag protein used in these experiments. The tissue was processed to localize labeling at the LM or EM levels, as described above. For EM observations, one block of tissue/animal at the level of the VApc and CM that contained dense anterograde labeling was taken out from slides and cut in ultrathin sections. These sections were used to study the pattern of synaptic connectivity and morphology of GPi terminals, as described below (see Analysis of Material).

vGluT1 immunostaining.—A specific vGluT1 antibody (Table 2; RRID:AB_2814813) was used to identify corticothalamic terminals in VApc and CM. The EM immunoperoxidase procedure to localize vGluT1 was the same as described above.

Analysis of the material

Striatal TH immunostaining intensity measurements.—The tissue was examined with a Leica DMRB light microscope (Leica Microsystems, Inc., Bannockburn, IL) and images were taken with a CCD camera (Leica DC 500; Leica IM50 software). For low magnification images, slides were scanned at 20× using a ScanScope CS scanning system (Aperio Technologies, Vista, CA). Digital representations of the slides were saved and analyzed using ImageScope software (Aperio Technologies). Using the ImageScope viewer software (Aperio), 0.7x magnification digital images of the stained tissue slides containing the caudate nucleus, putamen, or substantia nigra were selected and imported into ImageJ (NIH) (Schneider et al., 2012) for optical density measurements (Villalba and Smith, 2011; Villalba et al., 2014; Villalba et al., 2015). The images were converted into 16-bit grayscale format and inverted. Measurements of the intensity of labeling were obtained in two sections at the striatal and nigral levels from two groups of animals (control and MPTP-treated). In each section, the intensity of TH-staining was measured in four representative areas in each structure. To control for background staining, the optical density measurement in the internal capsule (for caudate and putamen) and cerebral peduncle (for SNc) was subtracted from the measurements. The resulting values were averaged in the MPTP-treated animals, and compared with similar data obtained in controls to determine the percent of TH

immunostaining loss in the striatum (caudate nucleus + putamen) and the substantia nigra in the MPTP-treated cases (Supplement Fig. 1g).

Density of vGAT and GAD67-staining.—Based on LM images of vGAT and GAD67-stained sections, the NIH ImageJ software was used to determine average densitometry values of vGAT and GAD67 immunolabeling intensity in the VApc and CM of control or MPTP-treated monkeys. The measured values were background-corrected by subtracting densitometry measurements from the internal capsule. To control for variability in the intensity of immunostaining between animals and runs of immunostaining, the densitometry measurement values in VApc and CM were then expressed relative to the intensity of immunostaining in the medial geniculate nucleus (MGN) or the ventral posteromedial nucleus (VPM), two thalamic nuclei with no known involvement in the pathophysiology of parkinsonism. We averaged densitometry measurements from regions of interest that covered approximately 85-90% of the total surface of the VApc, CM, MGN, or VPM. The ratios of VApc/MGN or CM/VPM average intensity measurements from 4-7 sections per animal were calculated for each animal, followed by statistical comparisons (t-test or Mann-Whitney test, as appropriate) of the mean VApc/MGN and CM/VPM ratios between control and parkinsonian monkeys.

Density of As, S1 and S2 terminals.—Ultrathin sections of VApc and CM tissue from the control and parkinsonian animals were examined in the EM. We collected >100 randomly chosen micrographs at 40,000X, from at least two blocks of tissue per animal from five control and three MPTP-treated animals in both the VApc and CM. The total number of micrographs analyzed in these experiments accounted for 1770 μm^2 and 2743 μm^2 of VApc in control and MPTP-treated monkeys, respectively, and 1770 μm^2 of CM in both control and MPTP-treated animals. To avoid counting the same terminals twice during our sampling, regions examined on single grids were distant from each other, and the distance between ultrathin sections cut from single blocks of tissue were spread apart by at least 2 μm. Using these micrographs, we distinguished different types of terminals in the thalamus based on their ultrastructural features, and determined their relative density (as terminals/μm^2; see Results section). To confirm the GABAergic nature of S1 and S2 terminals, sections from one control and one MPTP-treated monkey were immunostained for post-embedding GABA. Thus, micrographs from these animals were overlaid with gold particles indicative of GABA immunoreactivity (as described above). To ensure the specificity of the GABA labeling and categorize a terminal as GABAergic or not, we compared the density of gold particles over each terminal examined with that over putative glutamatergic terminals that formed asymmetric axo-spinous synapses in the same ultrathin sections. We arbitrarily considered that an ultrastructural element was positive for GABA if it contained more than two times the average density of gold particles than that over putative glutamatergic terminals. The density of terminals was compared between control and parkinsonian animals by One Way ANOVA; Holm-Sidak post-hoc testing for normally distributed data, and Dunn's Method post-hoc testing for data not normally distributed.

Size of glutamatergic terminals.—EM sections of vGluT1-stained material were used to compare the average cross-sectional area of corticothalamic terminals between control

and MPTP-treated monkeys. The cross-sectional area of at least 30 randomly selected vGluT1-labeled terminals that formed a clear asymmetric synapse in the VApc and CM of 3 control and 3 MPTP-treated monkeys was used. EM sections were selected and imported into ImageJ. The average cross-sectional areas of vGluT1-positive terminals for each animal were calculated at the level and the means were averaged amongst their respective group and compared between control and parkinsonian monkeys with t-tests.

Pattern of synaptic connectivity of GABAergic and glutamatergic terminals.— The post-synaptic targets of terminals were identified as cell bodies, large, medium or small dendrites (>1.0, 0.5-1.0 and <0.5 μm in diameter, respectively), based on their ultrastructural features and cross-sectional diameters (Peters et al., 1991). Dendrites of projection neurons were separated from dendrites of interneurons based on the presence of dendritic vesicles, which are exclusively found in interneurons (Hámori et al., 1974; Jones, 2002; Jones, 2007; Sherman and Friedlander, 1988; Sherman, 2004). The analysis included dendrites of projection neurons from at least 2 blocks per animal from 4-6 control and 3-5 MPTP-treated animals. The proportions of terminals in contact with each target were compared between control and parkinsonian animals for each pre-synaptic element by One Way ANOVA for normally distributed data, and Kruskal-Wallis analyses for data not normally distributed.

Relative prevalence of dendritic profiles.—We compared the relative density of large, medium and small dendrites in the VApc and CM between control and MPTP-treated monkeys. To do so, 25 randomly scanned electron micrographs of VApc and CM neuropil (25,000X) were analyzed in each animal. Dendrites were categorized by their cross-sectional diameter, as described above. The percentages of the different sizes of dendrites from each block of tissue were averaged for each animal. From there, the relative proportion of small-, medium- or large-sized dendrites in the VApc and CM was determined in control and parkinsonian monkeys.

Proportion of vGluT1-labeled terminals and of anterogradely labeled GPi terminals in contact with GABAergic interneurons.—The post-synaptic targets of 184 vGluT1-immunoreactive and 516 GFP-labeled GPi terminals were categorized as dendrites of projection neurons (no synaptic vesicle) or interneurons (with synaptic vesicles). The proportion of immunolabeled terminals in contact with each post-synaptic structure was determined and compared between control and parkinsonian monkeys. We collected data from 3-5 blocks per animal (vGluT1-labeled: 3 control and 3 MPTP-treated animals; labeled GPi terminals: 2 control and 2 MPTP-treated animals). Because of the low number of animals that could be used in this analysis, no statistics was performed on the data collected from GFP-labeled GPi terminals. Mann-Whitney Rank Sum test was used to determine significance between average number of vGluT1-labeled terminals that come in contact with projection neurons and interneurons in control and parkinsonian monkeys.

Data availability statement:

The data that support the findings of this study are available from the corresponding author upon reasonable request.

RESULTS

Nigrostriatal dopamine denervation in MPTP-treated monkeys

The depletion of the striatal dopaminergic innervation in the MPTP-treated animals was determined by assessing the decrease in the extent of TH immunoreactivity (TH-IR) in representative coronal sections of the pre-commissural, commissural, and post commissural striatum (Supplemental Fig. 1). All of the parkinsonian animals had decreased levels of TH-IR throughout the striatum (supplemental Fig. 1b, d, f). The quantification of the intensity of TH immunostaining in the pre- and post-commissural striatal levels showed an 83-91% lower level in MPTP-treated monkeys than in controls (Supplemental Fig. 1g). In the SN, a >90% lower level of TH-IR was observed in the MPTP-treated monkeys compared to controls (Supplemental Fig. 1g). These results are consistent with previous findings from our laboratory using the same animal model (Villalba et al., 2014).

GAD67 and vGAT Immunolabeling in VApc and CM

Thalamic tissue from six control and four MPTP-treated monkeys was immunostained for vGAT and GAD67 (Fig. 1a–d, f, h, i, k), and the density of these markers expressed as ratios to that found in neighboring MGN and VPM areas, as described in Methods. The boundaries of VApc and CM were determined using adjacent sections that were immunolabeled for calbindin D28K (Fig. 1g, j). We found that the VApc/MGN ratios for vGAT and GAD67 staining did not significantly differ between the MPTP-treated and control groups (Fig. 1e; $p = 0.091$, $p = 0.484$, respectively; t-test). Likewise, no significant difference was found in the CM/VPM ratios for vGAT and GAD67 staining between the two animal groups (Fig. 1I; $p = 0.429$, $p = 0.067$, respectively; t-test and Mann-Whitney Rank Sum test).

Types of GABAergic and glutamatergic terminals in VApc and CM

At the EM level, 3 types of axon terminals were identified in VApc and CM based on ultrastructural features reported in previous electron microscopic studies of the mammalian motor thalamus (Jones, 2007), and additional tract-tracing and immunohistochemical data presented in this study (Figs 2,3): (1) terminals forming asymmetric synapses (‘As’-type terminals; Fig. 3a, c), which putatively originate from the cerebral cortex, (2) terminals forming single symmetric synapses (‘S1’-type terminals; Fig. 3a–c), likely representing GABAergic inputs from the thalamic reticular nucleus (RTN) or GABAergic interneurons, and (3) terminals forming multiple symmetric synapses (‘S2’-type terminals; Fig. 2a–c), which originate from GABAergic neurons in GPi.

To further confirm that GPi was the source of S2 terminals, AAV5-eYFP was injected into the GPi (see supplement figure 2) of 2 control and 2 MPTP-treated monkeys, and the morphology of 82 anterogradely labeled terminals was examined in the EM. As expected, anterogradely labeled GPi terminals were large (1.0-3.0 μm in diameter) (Ilinsky et al., 1997; Kultas-Ilinsky et al., 1983; Kultas-Ilinsky et al., 1997; Shink et al., 1997), densely filled with mitochondria, and formed multiple axo-dendritic synapses (arrowheads) onto dendrites in VApc (Fig. 2a) and CM (Fig. 2c). To confirm the GABAergic nature of S1 and S2 terminals, ultrathin sections of VApc and CM from one control and one MPTP-treated monkey were processed for post-embedding GABA staining. In this material, all terminals

categorized as GABAergic S1 or S2 were overlaid with a density of gold particles that was at least twice as large as that over As glutamatergic terminals in the same ultrathin sections (Fig. 3).

Examples of the three categories of terminals forming axo-dendritic synapses in VApc and CM are shown in fig. 2 and 3. In figure 3A, the GABA-positive S1 terminal is in contact with a vesicle-filled dendrite of a putative GABAergic interneuron in the VApc of a control monkey (Fig. 3a). These data provide strong evidence that three major types of terminals in VApc and CM can be differentiated by their ultrastructural features in control and MPTP-treated parkinsonian monkeys.

Relative prevalence and preferred post-synaptic targets of GABAergic and glutamatergic terminals in the VApc and CM

To compare the relative abundance of As, S1 and S2 terminals in the thalamus of parkinsonian monkeys with that found in untreated animals, the density of each group of terminals was quantified in the VApc and CM of 5 control and 3 parkinsonian monkeys. Overall, the density of As terminals was significantly higher than that of S1 and S2 terminals in VApc of control and parkinsonian monkeys (Fig 4a; Control: $p<0.001$ for comparisons between the densities of As and S1 terminals, and of As and S2 terminals; MPTP: As vs S1: $p = 0.020$; As vs S2: $p = 0.004$; One Way ANOVA with Holm-Sidak post-hoc testing), and significantly higher than that of S2 terminals in CM of control monkeys (Fig. 5a; $p = 0.019$, One Way ANOVA with Dunn's Method). There was no significant group difference for S1 and S2 terminal densities between control and parkinsonian animals in both thalamic nuclei. However, compared to controls, the prevalence of As-type terminals was significantly lower in the VApc, but not in the CM, of the parkinsonian monkeys (Fig. 4a; $p<0.001$, One Way ANOVA with post-hoc Holm-Sidak testing).

To assess possible differences of the pattern of synaptic connectivity of As, S1 and S2 terminals between control and parkinsonian animals, the post-synaptic targets contacted by the three terminal sub-types were categorized as cell bodies, large (>1.0 um in diameter), medium (0.5-1.0 um in diameter) or small (<0.5 um in diameter) dendrites. The percentages of specific terminals in contact with each post-synaptic element was averaged and compared between control and parkinsonian animals with ANOVA. This analysis revealed no significant difference in the pattern of synaptic connectivity of As, S1, and S2 terminals in the VApc and CM between control and parkinsonian monkeys (Figs. 4b–d, 5b–d).

In both VApc and CM of control and parkinsonian monkeys, S2 terminals preferentially targeted large- and medium-sized dendrites, whereas As terminals were mainly located on medium-sized dendrites of thalamic cells (Figs. 4b–d, 5b–d). To determine whether this pattern of synaptic connections was random, and merely reflected the neuropil dendritic composition of the two thalamic nuclei, the average relative density of each dendrite type (i.e., small, medium, large) was assessed in the VApc and CM of 2 control and 2 parkinsonian monkeys. The relative abundance of each category of dendrites was closely similar between VApc and CM, and not significantly different between control and parkinsonian monkeys (Figs. 6a, c). In both thalamic nuclei and both conditions, small- (~50-63% of all dendrites) and medium- (~28-43%) sized dendrites accounted for most

dendritic profiles, while large-sized dendrites (~7-16%) were less common (Figs. 6a, c). To determine if the three types of terminals preferentially targeted a specific subset of dendrites, we calculated the ratio between the percent of each terminal subtype in contact with a specific population of dendrites over the average percentage of small-, medium- or large-sized dendrites in the VApc and CM of control (Fig. 6b, d) and MPTP-treated (Fig. 6b, d) monkeys. This analysis showed that S2 and As terminals were largely segregated on the proximal (diameter ≥ 0.5μm) vs distal (diameter ≤ 0.5μm) dendrites of VApc and CM neurons, respectively, in both control and parkinsonian monkeys (Fig. 6b, d), while S1 terminals were more homogeneously distributed along the whole somatodendritic domain of thalamic cells in each nucleus. In addition to this general pattern of synaptic connectivity, we found that in the VApc, very few S1 terminals contacted large-sized dendrites in the normal state, while the prevalence of such relationships was higher in parkinsonian animals (Fig. 6b). In the CM of MPTP-treated monkeys, synaptic contacts between S2 terminals and large-sized dendrites were uncommon (Fig. 6d).

Size of glutamatergic terminals in the VApc and CM of MPTP-treated monkeys

We measured the cross-sectional areas of vGluT1-positive (i.e., As, corticothalamic) terminals in the VApc and CM of control and parkinsonian monkeys. We randomly selected and examined 181 (VApc: 87, CM: 94) and 257 (VApc: 179, CM: 78) vGluT1-positive terminals at the level of the synapse in 3 control and 3 parkinsonian animals, respectively. This analysis revealed a significant increase in the average cross-sectional area of individual vGluT1-positive terminals in the VApc of MPTP-treated monkeys (Fig. 7a; $p<0.001$, t-test).

Corticothalamic and pallidothalamic synapses onto putative interneuron dendrites

We quantified the proportion of vGluT1-immunoreactive terminals and anterogradely labeled terminals from GPi in contact with interneurons in VApc and CM of control and parkinsonian monkeys. Dendrites of interneurons were differentiated from those of thalamocortical cells by their content in synaptic vesicles (Fig. 8a). Examples of direct synaptic contacts between the two types of thalamic afferent terminals and interneurons are shown in figures 9 and 10. In some instances, the pre-synaptic terminals that contacted the interneuron dendrites also formed synapses with neighboring dendrites of thalamocortical cells (Fig. 8a). The quantitative analysis of the synaptic connectivity of 184 vGluT1-positive and 516 GPi terminals suggested a trend towards a larger proportion of pallidothalamic (S2) terminals in contact with GABAergic interneurons in both thalamic nuclei of MPTP-treated parkinsonian monkeys compared with control animals (Fig. 9d, e). There was no significant difference between control and parkinsonian animals in the average percentage of vGluT1-labeled terminals that came in contact with projection neurons and interneurons (VApc: projection neurons: $p = 0.400$ and interneurons: $p = 0.400$; CM: projection neurons: $p = 0.700$ and interneurons: $p = 0.100$; Mann-Whitney Rank Sum Test).

DISCUSSION

We compared the relative prevalence, pattern of synaptic connectivity and ultrastructural features of the main glutamatergic and GABAergic inputs to the two thalamic-recipient nuclei of basal ganglia efferents, the VApc and CM, between control and MPTP-treated

parkinsonian monkeys. Three main observations were made: 1) the prevalence and overall pattern of synaptic connectivity of GABAergic terminals in VApc or CM was the same in the control and parkinsonian animals, 2) the prevalence of vGluT1-positive, putatively corticothalamic (i.e As), terminals was significantly reduced in the VApc of parkinsonian animals and 3) the cross-sectional area of the remaining vGluT1-immunoreactive terminals in the VApc of parkinsonian monkeys was significantly increased. Our findings also suggest a trend towards a larger proportion of pallidal terminals in contact with dendrites of GABAergic interneurons in parkinsonian monkeys compared with controls. The pruning and morphological changes of corticothalamic terminals seen in parkinsonian monkeys are reminiscent of previous findings from our group and others about corticostriatal and corticosubthalamic terminals in MPTP-treated monkeys, and in 6-hydroxydopamine-treated rodents (Chu et al., 2017; Day et al., 2006; Deutch, 2006; Ingham et al., 1998; Mathai and Smith, 2011; Mathai et al., 2015; Raju et al., 2008; Villalba et al., 2009; Villalba and Smith, 2010; Villalba and Smith, 2011; Villalba et al., 2015).

Synaptic Organization of VApc and CM in Control vs Parkinsonian Monkeys

The pattern of synaptic organization of the VApc and CM in normal monkeys is consistent with previous findings in rats, cats and monkeys (Bodor et al., 2008; Grofová and Rinvik, 1974; Ilinsky et al., 1999; Jones, 2007; Kultas-Ilinsky et al., 1983; Rovó et al., 2012; Sidibe et al., 1997; Smith et al., 1987). Similarly, the categorization of thalamic terminals in VApc and CM into three main groups (As,S1,S2) based on their chemical content (GABA vs. non-GABA), pattern of synaptic connections and ultrastructural features is also similar to previous observations (Bodor et al., 2008; Ilinsky et al., 1997; Ilinsky et al., 1999; Jones, 2007; Kultas-Ilinsky and Ilinsky, 1990; Kultas-Ilinsky et al., 1997; Sherman, 2004; Smith et al., 1987; Wanaverbecq et al., 2008). Although the exact source(s) of these terminals was not determined in the present study (except for showing that at least some S2 terminals belong to projections from GPi), data from previous tracing experiments published by our group and others suggest that most S1 terminals originate from the RTN, while the bulk of As terminals arise from the cerebral cortex (Jones, 2007; Kultas-Ilinsky et al., 1990; Smith et al., 1987). It is noteworthy that the VApc and CM receive other brainstem inputs (serotonergic, noradrenergic, dopaminergic, cholinergic) that were not considered in this study (Jones, 2007). The fact that many of these terminals do not form conventional synapses and do not display GABA or vGluT1 immunoreactivity (Jones, 2007), reduces the likelihood that they contribute substantially to the three main groups of terminals categorized in the present study.

Consistent with the previous literature (Balercia et al., 1996; Deschênes et al., 1998; Kakei et al., 2001; Kuo and Carpenter, 1973; Liu and Jones, 1999; Rouiller and Welker, 2000; Steriade, 2001; Wörgötter et al., 2002; Zhang and Jones, 2004), our data demonstrate that putative corticothalamic boutons (i.e., As terminals) are 4-6 times more abundant than GABAergic terminals from GPi and RTN in the VApc and CM. Based on their small size, general morphology and monosynaptic interactions with their postsynaptic targets, As terminals in VApc and CM are likely to be ‘modulatory’ (Bodor et al., 2008; Deschenes et al., 1994; Galvan et al., 2016; Rovó et al., 2012; Sherman, 2005). The significantly lower density of corticothalamic terminals in the VApc (but not in the CM) in parkinsonian

monkeys suggests that this system may undergo homeostatic (or maladaptive) plasticity and/or degeneration in the parkinsonian state (see below).

The general pattern of synaptic connections of As, S1 and S2 terminals with thalamocortical cells in the normal VApc and CM is consistent with previous reports. We found that corticothalamic (As) and RTN/interneuron (S1) terminals mainly target distal dendrites, while GPi terminals innervate preferentially the proximal dendrites and cell body of thalamocortical neurons (Grofova and Rinvik, 1974; Ilinsky and Kultas-Ilinsky, 1990; Jones, 2007; Kultas-Ilinsky et al., 1983; Sherman, 2004; Shink et al., 1997; Smith et al., 1987). Our findings did not reveal differences in these patterns of connectivity between control and parkinsonian animals. However, in the absence of detailed three-dimensional reconstructions, we cannot rule out the possibility of subtle changes of innervation.

The lack of differences in the prevalence and pattern of synaptic connections of GABAergic pallidothalamic synapses between the normal and parkinsonian animals does not exclude the possibility that the strength and functional properties of these synapses is affected in the parkinsonian state. Thus, the strength of the pallidothalamic system may be dynamically regulated by changes in the number, size, and proximity of synapses formed by individual pallidothalamic terminals, as previously described for other multisynaptic terminals (Bodor et al., 2008; Rovó et al., 2012; Wanaverbecq et al., 2008). Most importantly, such structural changes have also been described for pallidosubthalamic terminals in 6-OHDA-treated mice (Fan et al., 2012). Changes in the expression or the subunit composition of GABA receptors, mechanisms of GABA release and/or expression of GABA transporters must also be considered as mechanisms that may affect the pallidothalamic system in the parkinsonian state (and was not specifically examined in this study).

GABAergic innervation of CM in the parkinsonian state

The number of CM neurons is significantly decreased in PD patients and chronically MPTP-treated parkinsonian monkeys, compared to controls (Halliday et al., 2005; Halliday, 2009; Henderson et al., 2000a; Henderson et al., 2000b; Villalba et al., 2014). Surprisingly, despite the loss of CM neurons, the density of GABAergic terminals targeting such neurons was the same in normal and parkinsonian monkeys. This suggests that the GABAergic GPi and RTN terminals may preferentially target subpopulations of CM neurons that do not degenerate in the parkinsonian state. Findings from Halliday and colleagues suggest that non-parvalbumin (PV)-expressing neurons are particularly vulnerable in the CM of PD patients. Future studies that compare the innervation of PV- and non-PV-containing CM neurons by GABAergic afferents in normal and parkinsonian monkeys are obviously warranted. While the prevalence and pattern of synaptic connectivity of GABAergic terminals did not differ between the MPTP-treated and control monkeys, the proportion of single GPi terminals in contact with interneurons in the CM of MPTP-treated monkeys were higher than that found in controls. These findings are discussed in more detail in another section.

Plastic remodeling of the corticothalamic projection to VApc and CM in the parkinsonian state

Our findings demonstrate a lower prevalence of glutamatergic terminals in VApc, and a larger volume of these boutons in VApc and CM of parkinsonian monkeys, as compared to normal animals. These observations suggest that the corticothalamic system undergoes significant synaptic remodeling in the parkinsonian state.

In primates and rodents, corticothalamic glutamatergic terminals originate from pyramidal neurons in cortical layers V and VI. Although the physiological properties and morphology of these two populations of terminals have not been fully characterized in the motor thalamus, rodent data have provided strong evidence that these two groups of terminals are anatomically and functionally different in high order sensory nuclei. Corticothalamic projections from layer V pyramidal neurons are fast-conducting collaterals of long-range corticofugal axons that do not project to RTN (Jahanshahi et al., 1995; Rascol et al., 1994). In the pulvinar and medial dorsal nucleus, corticothalamic terminals of layer V neurons are relatively sparse, large, and form multiple asymmetric synapses with proximal dendrites and cell bodies of thalamocortical neurons and GABAergic interneurons (Callaway and Wiser, 1996; Deschenes et al., 1994; Paré and Smith, 1996; Rovó et al., 2012; Sherman, 2001; Sherman and Guillery, 2001; Sherman, 2005; Stepniewska et al., 2007). In contrast, corticothalamic terminals of layer VI neurons are abundant, small, and form synapses preferentially with distal dendrites of thalamic cells across the whole thalamus (Kakei et al., 2001; Rouiller and Welker, 2000; Rovó et al., 2012; Sirota et al., 2005). Electrophysiological studies have also demonstrated significant differences in the strength and functional properties of layer V and layer VI corticothalamic terminals in rodents, cats, and non-human primates (Deschenes et al., 1994; Kakei et al., 2001; Na et al., 1997; Rovó et al., 2012). Based on their high synaptic strength, layer V corticothalamic terminals are considered as potential “drivers” of high order thalamic nuclei, while layer VI terminals are seen as “modulators” of thalamic activity (Rovó et al., 2012; Sherman, 2012).

The basal ganglia-receiving nuclei of the primate motor thalamus receive inputs from layer V neurons in the primary motor cortex, the supplementary motor area, and the premotor cortex (McFarland and Haber, 2002; Rascol et al., 1992; Rouiller et al., 1998; Rouiller and Welker, 2000), but are devoid of large multisynaptic “driver-like” glutamatergic terminals (Goldberg et al., 2013; Jones, 2007; Percheron, 1997; Rovó et al., 2012). Data from our study using vGluT1 as a general marker of all corticothalamic terminals are consistent with these previous observations: none of the vGluT1-positive terminals in VApc and CM displayed the ultrastructural features of driver-like glutamatergic terminals in control and parkinsonian monkeys. Future studies using tracing and physiologic methods that allow differentiating layer V from layer VI corticothalamic projections to the VApc and CM of control and parkinsonian monkeys are needed to further examine the specific properties of these cortical inputs in the motor thalamus.

As stated above, we found that the abundance of vGluT1-containing cortical terminals in the VApc was significantly lower in parkinsonian monkeys than in untreated animals. This difference may be due to degeneration of corticothalamic neurons in motor cortices, specific loss of corticothalamic terminals in contact with thalamocortical cells, or from the loss of

thalamic neurons that receive cortical afferents. However, in contrast to the cell loss known to occur in CM, there is no neuronal loss in the VApc in parkinsonian humans and MPTP-treated monkeys (Halliday et al., 2005; Halliday, 2009; Henderson et al., 2000a; Villalba et al., 2014). Despite the profound neuronal loss in CM of parkinsonian monkeys (Villalba et al., 2014), the abundance of vGluT1-positive terminals was unchanged in the CM of MPTP-treated animals. These observations could be explained by a possible sprouting of new terminals from the remaining cortical axons or may suggest that CM neurons that degenerate in parkinsonian monkeys are not strongly innervated by the degenerated vGluT1-positive cortical terminals. It is noteworthy that a possible technical limitation may also explain our observations because our quantitative assessments of the prevalence of vGluT1-containing terminals in the CM of control and parkinsonian monkeys were not collected using unbiased stereological methods, thereby did not take into account the increased volume of the remaining vGluT1-positive terminals in the CM of parkinsonian monkeys.

Plasticity of Cortical and Pallidal Inputs to Putative GABAergic Interneurons in MPTP-treated Parkinsonian Monkeys

Up to 30% of all neurons in the primate VApc and CM are GABAergic interneurons (Ilinsky and Kultas-Ilinsky, 1990; Jones, 2007; Smith et al., 1987). In contrast, motor thalamic nuclei in rodents are practically devoid of GABAergic interneurons (Gabbott et al., 1986a; Gabbott et al., 1986b; Ohara et al., 1983). Limited data is available on the functional integration of the interneurons in the GABAergic microcircuitry of VApc and CM in primates (Ilinsky and Kultas-Ilinsky, 1990; Ilinsky et al., 1997; Ilinsky et al., 1999; Kultas-Ilinsky and Ilinsky, 1990; Kultas-Ilinsky and Ilinsky, 1991; Kultas-Ilinsky et al., 1997).

Because of the lack of a technical approach to selectively interrogate thalamic GABAergic interneurons in the primate brain, their physiologic responses and processing functions remain enigmatic. For instance, there is a tendency towards a larger proportion of single GPi terminals in contact with interneurons in the CM and VApc of parkinsonian monkeys than in controls. Although these observations must be statistically validated through further studies in a larger number of animals, it is noteworthy that a possible plastic reorganization of pallidal inputs to interneurons could act as a compensatory mechanism that counterbalances the increased inhibitory influences of GPi inputs onto thalamocortical cells. Such a change in synaptic organization could also alter other aspects of firing patterns in the thalamus (such as the level of synchrony between neighboring cells).

One caveat of these experiments is the fact that dendrites of GABAergic interneurons were recognized solely on the basis of the presence of synaptic vesicles. Although this ultrastructural feature is recognized as a unique characteristic of these interneurons (Jones, 2007), we cannot rule out that some of the dendritic profiles without synaptic vesicles in the present material also belong to interneurons. In addition, since S2 terminals are larger they are encountered more frequently and as a result have a higher proportion in single sections. Therefore, another caveat is the fact that we are unable to correct for the size of S2 terminals. Thus, the proportion of interneuron dendrites in contact with As, S1, and S2 terminals reported in the present study is likely to be an underestimate.

Conclusions

Together with previous findings from the striatum and the subthalamic nucleus, data from the present study demonstrate that changes in the prevalence, morphology and synaptic connectivity of glutamatergic and GABAergic terminals also occur in the basal ganglia-receiving thalamic nuclei in parkinsonian monkeys. Although much remains to be known about the functional significance of these structural changes, the possibility that they contribute to the complex pathophysiology of the basal-ganglia-thalamocortical loops in parkinsonism deserves further investigation.

Supplementary Material

Refer to Web version on PubMed Central for supplementary material.

Acknowledgements:

The authors thank J.F. Pare, S. Jenkins, H. Kelly, S. Lee, and P. Smith for technical assistance. This work was supported by NIH grants R01-NS083386, P50-NS098685 (Udall Center grant) and P51-OD011132 (Yerkes Center base grant).

REFERENCES

Akkal D, Dum RP, & Strick PL (2007). Supplementary motor area and presupplementary motor area: targets of basal ganglia and cerebellar output. J Neurosci, 27(40), 10659–10673. doi:10.1523/JNEUROSCI.3134-07.2007 [PubMed: 17913900]

Albin RL, Young AB, & Penney JB (1989). The functional anatomy of basal ganglia disorders. Trends Neurosci, 12(10), 366–375. [PubMed: 2479133]

Aymerich MS, Barroso-Chinea P, Perez-Manso M, Munoz-Patino AM, Moreno-Igoa M, Gonzalez-Hernandez T, & Lanciego JL (2006). Consequences of unilateral nigrostriatal denervation on the thalamostriatal pathway in rats. Eur J Neurosci, 23(8), 2099–2108. doi:10.1111/j.1460-9568.2006.04741.x [PubMed: 16630057]

Balercia G, Kultas-Ilinsky K, Bentivoglio M, & Ilinsky IA (1996). Neuronal and synaptic organization of the centromedian nucleus of the monkey thalamus: a quantitative ultrastructural study, with tract tracing and immunohistochemical observations. J Neurocytol, 25(4), 267–288. [PubMed: 8793732]

Bodor AL, Giber K, Rovo Z, Ulbert I, & Acsady L (2008). Structural correlates of efficient GABAergic transmission in the basal ganglia-thalamus pathway. J Neurosci, 28(12), 3090–3102. doi:10.1523/JNEUROSCI.5266-07.2008 [PubMed: 18354012]

Bogenpohl J, Galvan A, Hu X, Wichmann T, & Smith Y (2013). Metabotropic glutamate receptor 4 in the basal ganglia of parkinsonian monkeys: ultrastructural localization and electrophysiological effects of activation in the striatopallidal complex. Neuropharmacology, 66, 242–252. doi:10.1016/j.neuropharm.2012.05.017 [PubMed: 22634360]

Bosch-Bouju C, Smither RA, Hyland BI, & Parr-Brownlie LC (2014). Reduced reach-related modulation of motor thalamus neural activity in a rat model of Parkinson's disease. J Neurosci, 34(48), 15836–15850. doi:10.1523/JNEUROSCI.0893-14.2014 [PubMed: 25429126]

Callaway EM, & Wiser AK (1996). Contributions of individual layer 2-5 spiny neurons to local circuits in macaque primary visual cortex. Vis Neurosci, 13(5), 907–922. [PubMed: 8903033]

Charara A, Pare JF, Levey AI, & Smith Y (2005). Synaptic and extrasynaptic GABA-A and GABA-B receptors in the globus pallidus: an electron microscopic immunogold analysis in monkeys. Neuroscience, 131(4), 917–933. doi:10.1016/j.neuroscience.2004.12.004 [PubMed: 15749345]

Chen H, Zhuang P, Miao SH, Yuan G, Zhang YQ, Li JY, & Li YJ (2010). Neuronal firing in the ventrolateral thalamus of patients with Parkinson's disease differs from that with essential tremor. Chin Med J (Engl), 123(6), 695–701. [PubMed: 20368089]

Chu HY, McIver EL, Kovaleski RF, Atherton JF, & Bevan MD (2017). Loss of Hyperdirect Pathway Cortico-Subthalamic Inputs Following Degeneration of Midbrain Dopamine Neurons. Neuron, 95(6), 1306–1318 e1305. doi:10.1016/j.neuron.2017.08.038 [PubMed: 28910619]

Cox CL, Zhou Q, & Sherman SM (1998). Glutamate locally activates dendritic outputs of thalamic interneurons. Nature, 394(6692), 478–482. doi:10.1038/28855 [PubMed: 9697770]

Day M, Wang Z, Ding J, An X, Ingham CA, Shering AF, … Surmeier DJ (2006). Selective elimination of glutamatergic synapses on striatopallidal neurons in Parkinson disease models. Nat Neurosci, 9(2), 251–259. doi:10.1038/nn1632 [PubMed: 16415865]

DeLong MR (1971). Activity of pallidal neurons during movement. J Neurophysiol, 34(3), 414–427. doi:10.1152/jn.1971.34.3.414 [PubMed: 4997823]

DeLong MR (1990). Primate models of movement disorders of basal ganglia origin. Trends Neurosci, 13(7), 281–285. [PubMed: 1695404]

Deschenes M, Bourassa J, & Pinault D (1994). Corticothalamic projections from layer V cells in rat are collaterals of long-range corticofugal axons. Brain Res, 664(1-2), 215–219. doi:10.1016/0006-8993(94)91974-7 [PubMed: 7895031]

Deschenes M, Veinante P, & Zhang ZW (1998). The organization of corticothalamic projections: reciprocity versus parity. Brain Res Brain Res Rev, 28(3), 286–308. [PubMed: 9858751]

Deutch AY (2006). Striatal plasticity in parkinsonism: dystrophic changes in medium spiny neurons and progression in Parkinson's disease. J Neural Transm Suppl(70), 67–70.

Devergnas A, Chen E, Ma Y, Hamada I, Pittard D, Kammermeier S, … Wichmann T (2016). Anatomical localization of Cav3.1 calcium channels and electrophysiological effects of T-type calcium channel blockade in the motor thalamus of MPTP-treated monkeys. J Neurophysiol, 115(1), 470–485. doi:10.1152/jn.00858.2015 [PubMed: 26538609]

Devergnas A, Pittard D, Bliwise D, & Wichmann T (2014). Relationship between oscillatory activity in the cortico-basal ganglia network and parkinsonism in MPTP-treated monkeys. Neurobiol Dis, 68, 156–166. doi:10.1016/j.nbd.2014.04.004 [PubMed: 24768805]

Fan KY, Baufreton J, Surmeier DJ, Chan CS, & Bevan MD (2012). Proliferation of external globus pallidus-subthalamic nucleus synapses following degeneration of midbrain dopamine neurons. J Neurosci, 32(40), 13718–13728. doi:10.1523/JNEUROSCI.5750-11.2012 [PubMed: 23035084]

Gabbott PL, Somogyi J, Stewart MG, & Hamori J (1986a). GABA-immunoreactive neurons in the dorsal lateral geniculate nucleus of the rat: characterisation by combined Golgi-impregnation and immunocytochemistry. Exp Brain Res, 61(2), 311–322. doi:10.1007/bf00239521 [PubMed: 3512283]

Gabbott PL, Somogyi J, Stewart MG, & Hamori J (1986b). A quantitative investigation of the neuronal composition of the rat dorsal lateral geniculate nucleus using GABA-immunocytochemistry. Neuroscience, 19(1), 101–111. doi:10.1016/0306-4522(86)90008-4 [PubMed: 3537838]

Galvan A, Devergnas A, Pittard D, Masilamoni G, Vuong J, Daniels JS, … Wichmann T (2016). Lack of Antiparkinsonian Effects of Systemic Injections of the Specific T-Type Calcium Channel Blocker ML218 in MPTP-Treated Monkeys. ACS Chem Neurosci, 7(11), 1543–1551. doi:10.1021/acschemneuro.6b00186 [PubMed: 27596273]

Galvan A, Hu X, Rommelfanger KS, Pare JF, Khan ZU, Smith Y, & Wichmann T (2014). Localization and function of dopamine receptors in the subthalamic nucleus of normal and parkinsonian monkeys. J Neurophysiol, 112(2), 467–479. doi:10.1152/jn.00849.2013 [PubMed: 24760789]

Galvan A, Hu X, Smith Y, & Wichmann T (2010). Localization and function of GABA transporters in the globus pallidus of parkinsonian monkeys. Exp Neurol, 223(2), 505–515. doi:10.1016/j.expneurol.2010.01.018 [PubMed: 20138865]

Galvan A, Villalba RM, West SM, Maidment NT, Ackerson LC, Smith Y, & Wichmann T (2005). GABAergic modulation of the activity of globus pallidus neurons in primates: in vivo analysis of the functions of GABA receptors and GABA transporters. J Neurophysiol, 94(2), 990–1000. doi:10.1152/jn.00068.2005 [PubMed: 15829599]

Goldberg JH, Farries MA, & Fee MS (2013). Basal ganglia output to the thalamus: still a paradox. Trends Neurosci, 36(12), 695–705. doi:10.1016/j.tins.2013.09.001 [PubMed: 24188636]

Grofova I, & Rinvik E (1974). Cortical and pallidal projections to the nucleus ventralis lateralis thalami. Electron microscopical studies in the cat. Anat Embryol (Berl), 146(2), 113–132. [PubMed: 4618726]

Guehl D, Pessiglione M, Francois C, Yelnik J, Hirsch EC, Feger J, & Tremblay L (2003). Tremor-related activity of neurons in the 'motor' thalamus: changes in firing rate and pattern in the MPTP vervet model of parkinsonism. Eur J Neurosci, 17(11), 2388–2400. [PubMed: 12814370]

Gutierrez C, Cox CL, Rinzel J, & Sherman SM (2001). Dynamics of low-threshold spike activation in relay neurons of the cat lateral geniculate nucleus. J Neurosci, 21(3), 1022–1032. [PubMed: 11157087]

Gutierrez C, Cox CL, Rinzel J, & Sherman SM (2001). Dynamics of low-threshold spike activation in relay neurons of the cat lateral geniculate nucleus. J Neurosci, 21(3), 1022–1032. [PubMed: 11157087]

Hadipour-Niktarash A, Rommelfanger KS, Masilamoni GJ, Smith Y, &Wichmann T (2012). Extrastriatal D2-like receptors modulate basal ganglia pathways in normal and Parkinsonian monkeys. J Neurophysiol, 107(5), 1500–1512. doi:10.1152/jn.00348.2011 [PubMed: 22131382]

Halliday GM (2009). Thalamic changes in Parkinson's disease. Parkinsonism Relat Disord, 15 Suppl 3, S152–155. doi:10.1016/S1353-8020(09)70804-1 [PubMed: 20082979]

Halliday GM, Macdonald V, & Henderson JM (2005). A comparison of degeneration in motor thalamus and cortex between progressive supranuclear palsy and Parkinson's disease. Brain, 128(Pt 10), 2272–2280. doi:10.1093/brain/awh596 [PubMed: 16014651]

Hamori J, Pasik T, Pasik P, & Szentagothai J (1974). Triadic synaptic arrangements and their possible significance in the lateral geniculate nucleus of the monkey. Brain Res, 80(3), 379–393. doi:10.1016/0006-8993(74)91024-5 [PubMed: 4370837]

Henderson JM, Carpenter K, Cartwright H, & Halliday GM (2000a). Degeneration of the centre median-parafascicular complex in Parkinson's disease. Ann Neurol, 47(3), 345–352. [PubMed: 10716254]

Henderson JM, Carpenter K, Cartwright H, & Halliday GM (2000b). Loss of thalamic intralaminar nuclei in progressive supranuclear palsy and Parkinson's disease: clinical and therapeutic implications. Brain, 123 (Pt 7), 1410–1421. doi:10.1093/brain/123.7.1410 [PubMed: 10869053]

Hirsch EC, Perier C, Orieux G, Francois C, Feger J, Yelnik J, … Agid Y (2000). Metabolic effects of nigrostriatal denervation in basal ganglia. Trends Neurosci, 23(10 Suppl), S78–85. [PubMed: 11052224]

Ilinsky IA, Ambardekar AV, & Kultas-Ilinsky K (1999). Organization of projections from the anterior pole of the nucleus reticularis thalami (NRT) to subdivisions of the motor thalamus: light and electron microscopic studies in the rhesus monkey. J Comp Neurol, 409(3), 369–384. [PubMed: 10379824]

Ilinsky IA, & Kultas-Ilinsky K (1990). Fine structure of the magnocellular subdivision of the ventral anterior thalamic nucleus (VAmc) of Macaca mulatta: I. Cell types and synaptology. J Comp Neurol, 294(3), 455–478. doi:10.1002/cne.902940313 [PubMed: 2341621]

Ilinsky IA, Yi H, & Kultas-Ilinsky K (1997). Mode of termination of pallidal afferents to the thalamus: a light and electron microscopic study with anterograde tracers and immunocytochemistry in Macaca mulatta. J Comp Neurol, 386(4), 601–612. [PubMed: 9378854]

Inase M, Tokuno H, Nambu A, Akazawa T, & Takada M (1996). Origin of thalamocortical projections to the presupplementary motor area (pre-SMA) in the macaque monkey. Neurosci Res, 25(3), 217–227. [PubMed: 8856718]

Ingham CA, Hood SH, Taggart P, & Arbuthnott GW (1998). Plasticity of synapses in the rat neostriatum after unilateral lesion of the nigrostriatal dopaminergic pathway. J Neurosci, 18(12), 4732–4743. [PubMed: 9614247]

Jahanshahi M, Jenkins IH, Brown RG, Marsden CD, Passingham RE, & Brooks DJ (1995). Self-initiated versus externally triggered movements. I. An investigation using measurement of regional cerebral blood flow with PET and movement-related potentials in normal and Parkinson's disease subjects. Brain, 118 (Pt 4), 913–933. doi: 10.1093/brain/118.4.913 [PubMed: 7655888]

Jones EG (2002). Thalamic organization and function after Cajal. Prog Brain Res, 136, 333–357. [PubMed: 12143393]

Jones EG (2007) The Thalamus, Volumes 1 and 2, Cambridge University Press.

Kakei S, Na J, & Shinoda Y (2001). Thalamic terminal morphology and distribution of single corticothalamic axons originating from layers 5 and 6 of the cat motor cortex. J Comp Neurol, 437(2), 170–185. [PubMed: 11494250]

Kammermeier S, Pittard D, Hamada I, & Wichmann T (2016). Effects of high-frequency stimulation of the internal pallidal segment on neuronal activity in the thalamus in parkinsonian monkeys. J Neurophysiol, 116(6), 2869–2881. doi:10.1152/jn.00104.2016 [PubMed: 27683881]

Kliem MA, Maidment NT, Ackerson LC, Chen S, Smith Y, & Wichmann T (2007). Activation of nigral and pallidal dopamine D1-like receptors modulates basal ganglia outflow in monkeys. J Neurophysiol, 98(3), 1489–1500. doi:10.1152/jn.00171.2007 [PubMed: 17634344]

Kliem MA, Pare JF, Khan ZU, Wichmann T, & Smith Y (2009). Comparative Ultrastructural Analysis of D1 and D5 Dopamine Receptor Distribution in the Substantia Nigra and Globus Pallidus of Monkeys. Adv Behav Biol, 58, 239–253. doi:10.1007/978-1-4419-0340-2_19 [PubMed: 19750130]

Kliem MA, & Wichmann T (2004). A method to record changes in local neuronal discharge in response to infusion of small drug quantities in awake monkeys. J Neurosci Methods, 138(1-2), 45–49. doi:10.1016/j.jneumeth.2004.03.015 [PubMed: 15325110]

Kultas-Ilinsky K, Ilinsky I, Warton S, & Smith KR (1983). Fine structure of nigral and pallidal afferents in the thalamus: an EM autoradiography study in the cat. J Comp Neurol, 216(4), 390–405. doi:10.1002/cne.902160405 [PubMed: 6308072]

Kultas-Ilinsky K, & Ilinsky IA (1990). Fine structure of the magnocellular subdivision of the ventral anterior thalamic nucleus (VAmc) of Macaca mulatta: II. Organization of nigrothalamic afferents as revealed with EM autoradiography. J Comp Neurol, 294(3), 479–489. doi:10.1002/cne.902940314 [PubMed: 2341622]

Kultas-Ilinsky K, & Ilinsky IA (1991). Fine structure of the ventral lateral nucleus (VL) of the Macaca mulatta thalamus: cell types and synaptology. J Comp Neurol, 314(2), 319–349. doi:10.1002/cne.903140209 [PubMed: 1723998]

Kultas-Ilinsky K, Reising L, Yi H, & Ilinsky IA (1997). Pallidal afferent territory of the Macaca mulatta thalamus: neuronal and synaptic organization of the VAdc. J Comp Neurol, 386(4), 573–600. [PubMed: 9378853]

Kuo JS, & Carpenter MB (1973). Organization of pallidothalamic projections in the rhesus monkey. J Comp Neurol, 151(3), 201–236. doi:10.1002/cne.901510302 [PubMed: 4126710]

Lanciego JL, Lopez IP, Rico AJ, Aymerich MS, Perez-Manso M, Conte L, … Barroso-Chinea P (2009). The search for a role of the caudal intralaminar nuclei in the pathophysiology of Parkinson's disease. Brain Res Bull, 78(2-3), 55–59. doi:10.1016/j.brainresbull.2008.08.008 [PubMed: 18790023]

Lanciego JL, & Vazquez A (2012). The basal ganglia and thalamus of the long-tailed macaque in stereotaxic coordinates. A template atlas based on coronal, sagittal and horizontal brain sections. Brain Struct Funct, 217(2), 613–666. doi:10.1007/s00429-011-0370-5 [PubMed: 22179107]

Levitt JB, Schumer RA, Sherman SM, Spear PD, & Movshon JA (2001). Visual response properties of neurons in the LGN of normally reared and visually deprived macaque monkeys. J Neurophysiol, 85(5), 2111–2129. doi:10.1152/jn.2001.85.5.2111 [PubMed: 11353027]

Liu XB, & Jones EG (1999). Predominance of corticothalamic synaptic inputs to thalamic reticular nucleus neurons in the rat. J Comp Neurol, 414(1), 67–79. [PubMed: 10494079]

Magnin M, Morel A, & Jeanmonod D (2000). Single-unit analysis of the pallidum, thalamus and subthalamic nucleus in parkinsonian patients. Neuroscience, 96(3), 549–564. doi:10.1016/s0306-4522(99)00583-7 [PubMed: 10717435]

Masilamoni G, Votaw J, Howell L, Villalba RM, Goodman M, Voll RJ, … Smith Y (2010). (18)F-FECNT: validation as PET dopamine transporter ligand in parkinsonism. Exp Neurol, 226(2), 265–273. doi:10.1016/j.expneurol.2010.08.024 [PubMed: 20832405]

Masilamoni GJ, Bogenpohl JW, Alagille D, Delevich K, Tamagnan G, Votaw JR, … Smith Y (2011). Metabotropic glutamate receptor 5 antagonist protects dopaminergic and noradrenergic neurons from degeneration in MPTP-treated monkeys. Brain, 134(Pt 7), 2057–2073. doi:10.1093/brain/awr137 [PubMed: 21705423]

Masilamoni GJ, & Smith Y (2018). Chronic MPTP administration regimen in monkeys: a model of dopaminergic and non-dopaminergic cell loss in Parkinson's disease. J Neural Transm (Vienna), 125(3), 337–363. doi:10.1007/s00702-017-1774-z [PubMed: 28861737]

Mathai A, Ma Y, Pare JF, Villalba RM, Wichmann T, & Smith Y (2015). Reduced cortical innervation of the subthalamic nucleus in MPTP-treated parkinsonian monkeys. Brain, 138(Pt 4), 946–962. doi:10.1093/brain/awv018 [PubMed: 25681412]

Mathai A, & Smith Y (2011). The corticostriatal and corticosubthalamic pathways: two entries, one target. So what? Front Syst Neurosci, 5, 64. doi:10.3389/fnsys.2011.00064 [PubMed: 21866224]

McFarland NR, & Haber SN (2000). Convergent inputs from thalamic motor nuclei and frontal cortical areas to the dorsal striatum in the primate. J Neurosci, 20(10), 3798–3813. [PubMed: 10804220]

McFarland NR, & Haber SN (2001). Organization of thalamostriatal terminals from the ventral motor nuclei in the macaque. J Comp Neurol, 429(2), 321–336. [PubMed: 11116223]

McFarland NR, & Haber SN (2002). Thalamic relay nuclei of the basal ganglia form both reciprocal and nonreciprocal cortical connections, linking multiple frontal cortical areas. J Neurosci, 22(18), 8117–8132. [PubMed: 12223566]

Mitchell IJ, Clarke CE, Boyce S, Robertson RG, Peggs D, Sambrook MA, & Crossman AR (1989). Neural mechanisms underlying parkinsonian symptoms based upon regional uptake of 2-deoxyglucose in monkeys exposed to 1-methyl-4-phenyl-1,2,3,6-tetrahydropyridine. Neuroscience, 32(1), 213–226. doi:10.1016/0306-4522(89)90120-6 [PubMed: 2586750]

Molnar GF, Pilliar A, Lozano AM, & Dostrovsky JO (2005). Differences in neuronal firing rates in pallidal and cerebellar receiving areas of thalamus in patients with Parkinson's disease, essential tremor, and pain. J Neurophysiol, 93(6), 3094–3101. doi:10.1152/jn.00881.2004 [PubMed: 15703231]

Na J, Kakei S, & Shinoda Y (1997). Cerebellar input to corticothalamic neurons in layers V and VI in the motor cortex. Neurosci Res, 28(1), 77–91. [PubMed: 9179883]

Ni ZG, Gao DM, Benabid AL, & Benazzouz A (2000). Unilateral lesion of the nigrostriatal pathway induces a transient decrease of firing rate with no change in the firing pattern of neurons of the parafascicular nucleus in the rat. Neuroscience, 101(4), 993–999. doi:10.1016/s0306-4522(00)00337-7 [PubMed: 11113348]

Ohara PT, Lieberman AR, Hunt SP, & Wu JY (1983). Neural elements containing glutamic acid decarboxylase (GAD) in the dorsal lateral geniculate nucleus of the rat; immunohistochemical studies by light and electron microscopy. Neuroscience, 8(2), 189–211. doi:10.1016/0306-4522(83)90060-x [PubMed: 6341876]

Orieux G, Francois C, Feger J, Yelnik J, Vila M, Ruberg M, … Hirsch EC (2000). Metabolic activity of excitatory parafascicular and pedunculopontine inputs to the subthalamic nucleus in a rat model of Parkinson's disease. Neuroscience, 97(1), 79–88. doi:10.1016/s0306-4522(00)00011-7 [PubMed: 10771341]

Pare D, & Smith Y (1996). Thalamic collaterals of corticostriatal axons: their termination field and synaptic targets in cats. J Comp Neurol, 372(4), 551–567. doi:10.1002/(SICI)1096-9861(19960902)372:4<551::AID-CNE5>3.0.CO;2-3 [PubMed: 8876453]

Parent A, Mackey A, Smith Y, & Boucher R (1983). The output organization of the substantia nigra in primate as revealed by a retrograde double labeling method. Brain Res Bull, 10(4), 529–537. doi:10.1016/0361-9230(83)90151-x [PubMed: 6305462]

Parent M, Levesque M, & Parent A (2001). Two types of projection neurons in the internal pallidum of primates: single-axon tracing and three-dimensional reconstruction. J Comp Neurol, 439(2), 162–175. [PubMed: 11596046]

Parent M, & Parent A (2004). The pallidofugal motor fiber system in primates. Parkinsonism Relat Disord, 10(4), 203–211. doi: 10.1016/j.parkreldis.2004.02.007 [PubMed: 15120094]

Percheron G (1997). The motor thalamus. J Neurosurg, 87(6), 981–982. [PubMed: 9384418]

Pessiglione M, Guehl D, Rolland AS, Francois C, Hirsch EC, Feger J, & Tremblay L (2005). Thalamic neuronal activity in dopamine-depleted primates: evidence for a loss of functional segregation within basal ganglia circuits. J Neurosci, 25(6), 1523–1531. doi:10.1523/JNEUROSCI.4056-04.2005 [PubMed: 15703406]

Raeva S, Vainberg N, & Dubinin V (1999). Analysis of spontaneous activity patterns of human thalamic ventrolateral neurons and their modifications due to functional brain changes. Neuroscience, 88(2), 365–376. doi:10.1016/s0306-4522(98)00228-0 [PubMed: 10197760]

Raju DV, Ahern TH, Shah DJ, Wright TM, Standaert DG, Hall RA, & Smith Y (2008). Differential synaptic plasticity of the corticostriatal and thalamostriatal systems in an MPTP-treated monkey model of parkinsonism. Eur J Neurosci, 27(7), 1647–1658. doi:10.1111/j.1460-9568.2008.06136.x [PubMed: 18380666]

Ramcharan EJ, Gnadt JW, & Sherman SM (2001). The effects of saccadic eye movements on the activity of geniculate relay neurons in the monkey. Vis Neurosci, 18(2), 253–258. doi:10.1017/s0952523801182106 [PubMed: 11417800]

Rascol O, Sabatini U, Chollet F, Celsis P, Montastruc JL, Marc-Vergnes JP, & Rascol A (1992). Supplementary and primary sensory motor area activity in Parkinson's disease. Regional cerebral blood flow changes during finger movements and effects of apomorphine. Arch Neurol, 49(2), 144–148. doi:10.1001/archneur.1992.00530260044017 [PubMed: 1736846]

Rascol O, Sabatini U, Chollet F, Fabre N, Senard JM, Montastruc JL, … Rascol A (1994). Normal activation of the supplementary motor area in patients with Parkinson's disease undergoing long-term treatment with levodopa. J Neurol Neurosurg Psychiatry, 57(5), 567–571. doi:10.1136/jnnp.57.5.567 [PubMed: 8201325]

Rolland AS, Herrero MT, Garcia-Martinez V, Ruberg M, Hirsch EC, & Francois C (2007). Metabolic activity of cerebellar and basal ganglia-thalamic neurons is reduced in parkinsonism. Brain, 130(Pt 1), 265–275. doi:10.1093/brain/awl337 [PubMed: 17148469]

Rouiller EM, Tanne J, Moret V, Kermadi I, Boussaoud D, & Welker E (1998). Dual morphology and topography of the corticothalamic terminals originating from the primary, supplementary motor, and dorsal premotor cortical areas in macaque monkeys. J Comp Neurol, 396(2), 169–185. [PubMed: 9634140]

Rouiller EM, & Welker E (2000). A comparative analysis of the morphology of corticothalamic projections in mammals. Brain Res Bull, 53(6), 727–741. doi:10.1016/s0361-9230(00)00364-6 [PubMed: 11179837]

Rovo Z, Ulbert I, & Acsady L (2012). Drivers of the primate thalamus. J Neurosci, 32(49), 17894–17908. doi:10.1523/JNEUROSCI.2815-12.2012 [PubMed: 23223308]

Sadikot AF, Parent A, & Francois C (1992). Efferent connections of the centromedian and parafascicular thalamic nuclei in the squirrel monkey: a PHA-L study of subcortical projections. J Comp Neurol, 315(2), 137–159. doi:10.1002/cne.903150203 [PubMed: 1372010]

Sakai ST, Inase M, & Tanji J (1999). Pallidal and cerebellar inputs to thalamocortical neurons projecting to the supplementary motor area in Macaca fuscata: a triple-labeling light microscopic study. Anat Embryol (Berl), 199(1), 9–19. [PubMed: 9924930]

Sarnthein J, & Jeanmonod D (2007). High thalamocortical theta coherence in patients with Parkinson's disease. J Neurosci, 27(1), 124–131. doi:10.1523/JNEUROSCI.2411-06.2007 [PubMed: 17202479]

Schell GR, & Strick PL (1984). The origin of thalamic inputs to the arcuate premotor and supplementary motor areas. J Neurosci, 4(2), 539–560. [PubMed: 6199485]

Schneider CA, Rasband WS, & Eliceiri KW (2012). NIH Image to ImageJ: 25 years of image analysis. Nat Methods, 9(7), 671–675. [PubMed: 22930834]

Schneider JS, & Rothblat DS (1996). Alterations in intralaminar and motor thalamic physiology following nigrostriatal dopamine depletion. Brain Res, 742(1-2), 25–33. doi:10.1016/s0006-8993(96)00988-2 [PubMed: 9117401]

Sherman SM (2001). Thalamic relay functions. Prog Brain Res, 134, 51–69. doi:10.1016/s0079-6123(01)34005-0 [PubMed: 11702563]

Sherman SM (2004). Interneurons and triadic circuitry of the thalamus. Trends Neurosci, 27(11), 670–675. doi:10.1016/j.tins.2004.08.003 [PubMed: 15474167]

Sherman SM (2005). Thalamic relays and cortical functioning. Prog Brain Res, 149, 107–126. doi:10.1016/S0079-6123(05)49009-3 [PubMed: 16226580]

Sherman SM (2012). Thalamocortical interactions. Curr Opin Neurobiol, 22(4), 575–579. doi:10.1016/j.conb.2012.03.005 [PubMed: 22498715]

Sherman SM, & Friedlander MJ (1988). Identification of X versus Y properties for interneurons in the A-laminae of the cat's lateral geniculate nucleus. Exp Brain Res, 73(2), 384–392. doi:10.1007/bf00248231 [PubMed: 3215314]

Sherman SM & Guillery RW (2001) Exploring the Thalamus, Academic Press, Sa Diego

Shindo K, Shima K, & Tanji J (1995). Spatial distribution of thalamic projections to the supplementary motor area and the primary motor cortex: a retrograde multiple labeling study in the macaque monkey. J Comp Neurol, 357(1), 98–116. doi:10.1002/cne.903570110 [PubMed: 7673471]

Shink E, Sidibe M, & Smith Y (1997). Efferent connections of the internal globus pallidus in the squirrel monkey: II. Topography and synaptic organization of pallidal efferents to the pedunculopontine nucleus. J Comp Neurol, 382(3), 348–363. [PubMed: 9183698]

Sidibe M, & Smith Y (1996). Differential synaptic innervation of striatofugal neurones projecting to the internal or external segments of the globus pallidus by thalamic afferents in the squirrel monkey. J Comp Neurol, 365(3), 445–465. doi:10.1002/(SICI)1096-9861(19960212)365:3<445::AID-CNE8>3.0.CO;2-4 [PubMed: 8822181]

Sirota MG, Swadlow HA, & Beloozerova IN (2005). Three channels of corticothalamic communication during locomotion. J Neurosci, 25(25), 5915–5925. doi:10.1523/JNEUROSCI.0489-05.2005 [PubMed: 15976080]

Smith Y, Galvan A, Ellender TJ, Doig N, Villalba RM, Huerta-Ocampo I, … Bolam JP (2014). The thalamostriatal system in normal and diseased states. Front Syst Neurosci, 8, 5. doi:10.3389/fnsys.2014.00005 [PubMed: 24523677]

Smith Y, & Parent A (1986). Differential connections of caudate nucleus and putamen in the squirrel monkey (Saimiri sciureus). Neuroscience, 18(2), 347–371. doi:10.1016/0306-4522(86)90159-4 [PubMed: 3736862]

Smith Y, Seguela P, & Parent A (1987). Distribution of GABA-immunoreactive neurons in the thalamus of the squirrel monkey (Saimiri sciureus). Neuroscience, 22(2), 579–591. doi:10.1016/0306-4522(87)90355-1 [PubMed: 3670598]

Stepniewska I, Sakai ST, Qi HX, & Kaas JH (2003). Somatosensory input to the ventrolateral thalamic region in the macaque monkey: potential substrate for parkinsonian tremor. J Comp Neurol, 455(3), 378–395. doi:10.1002/cne.10499 [PubMed: 12483689]

Steriade M (2001). Impact of network activities on neuronal properties in corticothalamic systems. J Neurophysiol, 86(1), 1–39. doi:10.1152/jn.2001.86.1.1 [PubMed: 11431485]

Tokuno H, Kimura M, & Tanji J (1992). Pallidal inputs to thalamocortical neurons projecting to the supplementary motor area: an anterograde and retrograde double labeling study in the macaque monkey. Exp Brain Res, 90(3), 635–638.doi:10.1007/bf00230949 [PubMed: 1385203]

Villalba RM, Lee H, & Smith Y (2009). Dopaminergic denervation and spine loss in the striatum of MPTP-treated monkeys. Exp Neurol, 215(2), 220–227. doi:10.1016/j.expneurol.2008.09.025 [PubMed: 18977221]

Villalba RM, Mathai A, & Smith Y (2015). Morphological changes of glutamatergic synapses in animal models of Parkinson's disease. Front Neuroanat, 9, 117. doi:10.3389/fnana.2015.00117 [PubMed: 26441550]

Villalba RM, & Smith Y (2010). Striatal spine plasticity in Parkinson's disease. Front Neuroanat, 4, 133. doi:10.3389/fnana.2010.00133 [PubMed: 21179580]

Villalba RM, & Smith Y (2011). Differential structural plasticity of corticostriatal and thalamostriatal axo-spinous synapses in MPTP-treated Parkinsonian monkeys. J Comp Neurol, 519(5), 989–1005.doi:10.1002/cne.22563 [PubMed: 21280048]

Villalba RM, Wichmann T, & Smith Y (2014). Neuronal loss in the caudal intralaminar thalamic nuclei in a primate model of Parkinson's disease. Brain Struct Fund, 219(1), 381–394. doi:10.1007/s00429-013-0507-9

Wanaverbecq N, Bodor AL, Bokor H, Slezia A, Luthi A, & Acsady L (2008). Contrasting the functional properties of GABAergic axon terminals with single and multiple synapses in the thalamus. J Neurosci, 28(46), 11848–11861. doi:10.1523/JNEUROSCI.3183-08.2008 [PubMed: 19005050]

Wang S, Bickford ME, Van Horn SC, Erisir A, Godwin DW, & Sherman SM (2001). Synaptic targets of thalamic reticular nucleus terminals in the visual thalamus of the cat. J Comp Neurol, 440(4), 321–341. doi:10.1002/cne.1389 [PubMed: 11745627]

Wang S, Bickford ME, Van Horn SC, Erisir A, Godwin DW, & Sherman SM (2001). Synaptic targets of thalamic reticular nucleus terminals in the visual thalamus of the cat. J Comp Neurol, 440(4), 321–341. doi:10.1002/cne.1389 [PubMed: 11745627]

Wichmann T, Kliem MA, & DeLong MR (2001). Antiparkinsonian and behavioral effects of inactivation of the substantia nigra pars reticulata in hemiparkinsonian primates. Exp Neurol, 167(2), 410–424. doi:10.1006/exnr.2000.7572 [PubMed: 11161630]

Wichmann T, & Soares J (2006). Neuronal firing before and after burst discharges in the monkey basal ganglia is predictably patterned in the normal state and altered in parkinsonism. J Neurophysiol, 95(4), 2120–2133. doi:10.1152/jn.01013.2005 [PubMed: 16371459]

Worgotter F, Eyding D, Macklis JD, & Funke K (2002). The influence of the corticothalamic projection on responses in thalamus and cortex. Philos Trans R Soc Lond B Biol Sci, 357(1428), 1823–1834. doi:10.1098/rstb.2002.1159 [PubMed: 12626015]

Zhang L, & Jones EG (2004). Corticothalamic inhibition in the thalamic reticular nucleus. J Neurophysiol, 91(2), 759–766. doi:10.1152/jn.00624.2003 [PubMed: 14586030]

Zirh TA, Lenz FA, Reich SG, & Dougherty PM (1998). Patterns of bursting occurring in thalamic cells during parkinsonian tremor. Neuroscience, 83(1), 107–121. doi: 10.1016/s0306-4522(97)00295 [PubMed: 9466402]

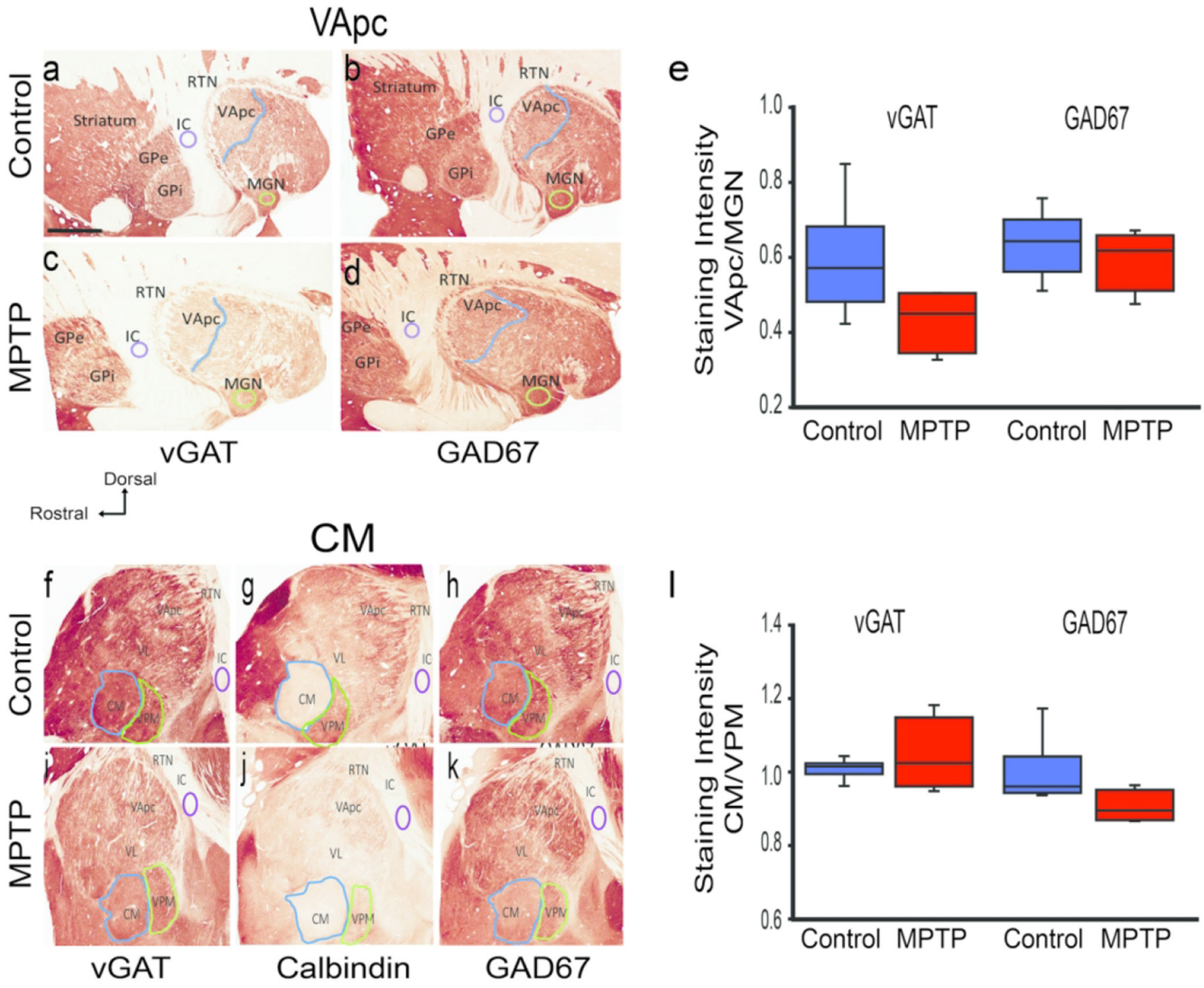

Fig. 1.

Vesicular GABAergic Transporter (vGAT) and Glutamic acid decarboxylase 67 (GAD67) immunoreactivity (IR) in the ventral anterior parvocellular part (VApc) and centromedian (CM) thalamic nuclei. Sagittal sections of the VApc (**a-d**) and CM (**f-k**) in control (n=6) and MPTP-treated (n=4) animals processed for vGAT-IR, GAD67-IR, and calbindin. (**e,l**) Intensity of vGAT-IR and GAD-67 IR in the VApc and CM of control and MPTP-treated monkeys, expressed as ratio of staining intensity (**e**) VApc/medial geniculate nucleus (MGN) or (**I**) CM/ventral posteromedial nucleus (VPM). *GPe*, *GPi* Globus pallidus external, internal (respectively), *RTN* reticular thalamic nucleus, *IC* internal capsule, *VL* ventral lateral thalamic nucleus. Data are expressed as mean± SEM. *Scale bar* in **a** (applies to **b-k**) = 4mm.

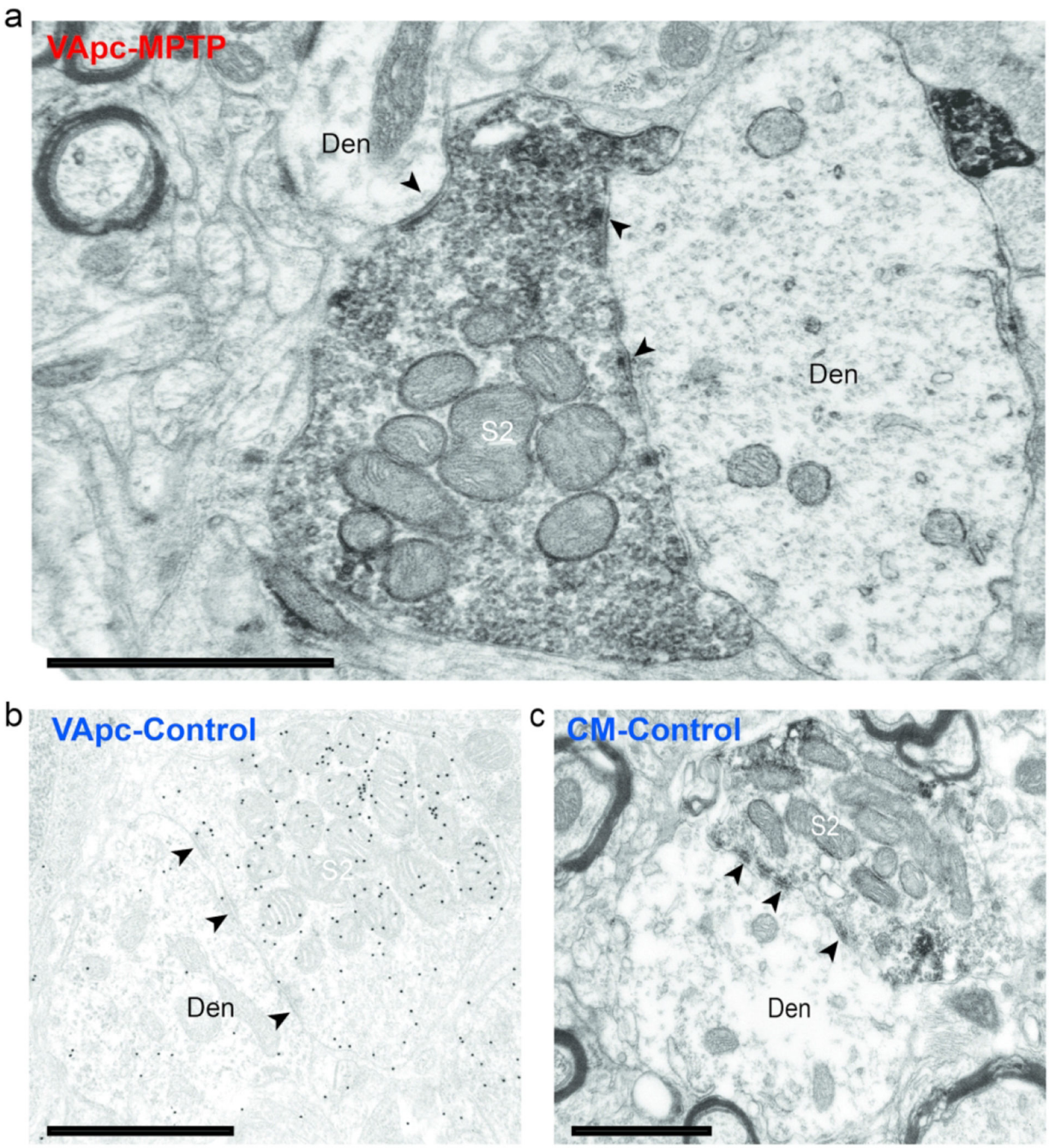

Fig. 2.

S2-type terminals in the VApc and CM of control and MPTP-treated monkeys. (**a,c**) Electron micrograph of an EYFP-containing GPi (S2-type) terminal forming multiple synapses (arrowheads) onto dendrites in the (**a**) VApc of a MPTP-treated monkey and (**c**) CM of a control animal. (**b**) Electron micrograph of a S2-like GABA-labeled terminal forming multiple synapses onto a dendrite in the VApc of a control monkey. In a and c, the GFP immunostaining was revealed with immunoperoxidase (dense deposits), in b, GABA

labeling was localized with immunogold particles (small black dots). Black arrowheads = individual synapses. *Scale bars* correspond to 1 μm.

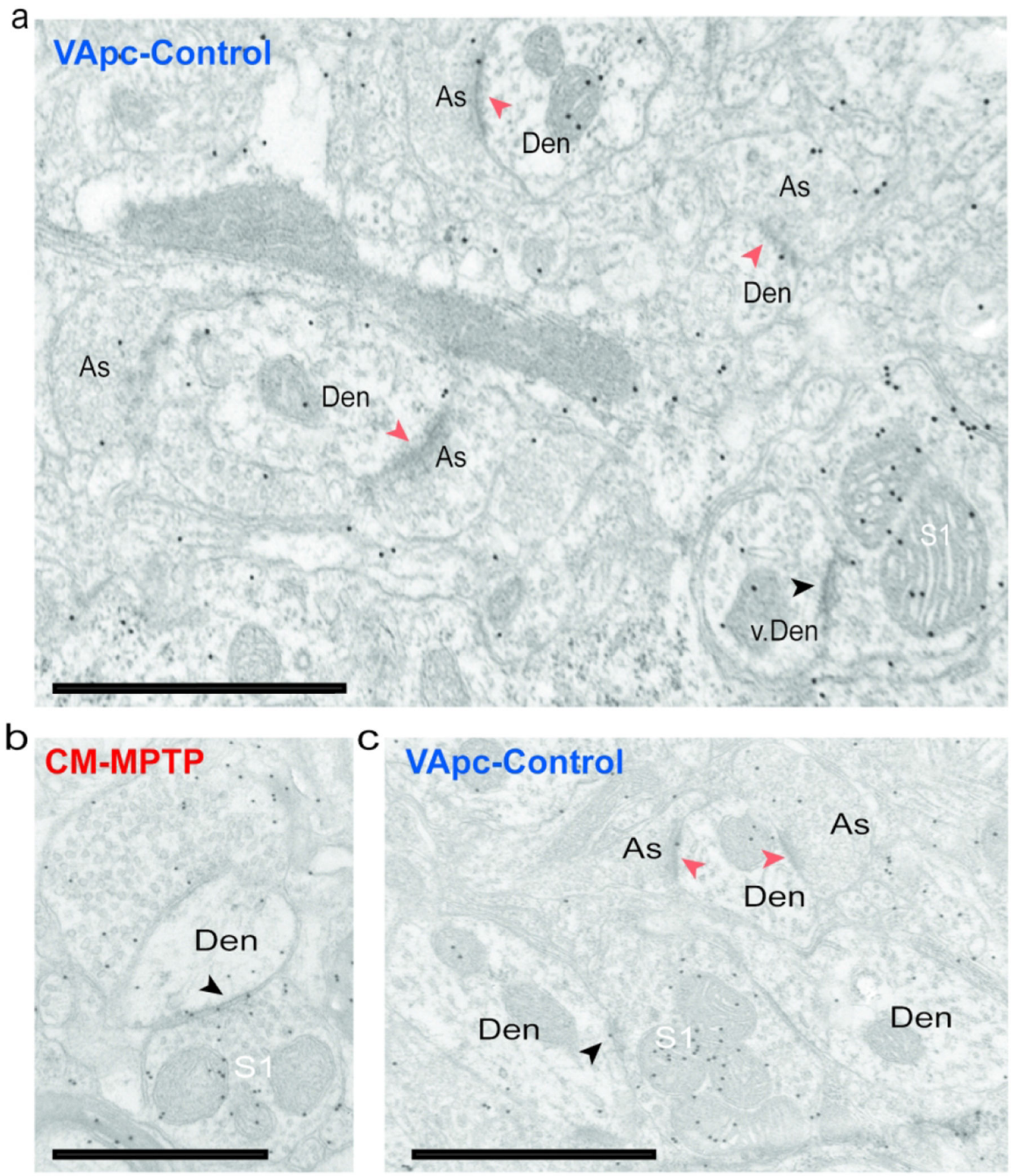

Fig. 3.

S1 and As-type terminals in the VApc and CM in normal and MPTP-treated monkeys. (**a**) Post-embedding immunogold GABA labeling that shows GABA-negative As-type terminals in contact with small- and medium-sized dendrites (Den) and a GABA-positive S1 terminal in contact with a vesicle-filled interneuron's dendrite (v. Den) in the VApc of a control monkey. (**b**) S1-type terminal in the CM of an MPTP-treated monkey in contact with a medium-sized dendrite. (**c**) GABA-positive S1-type terminal in the VApc of a normal monkey in contact with a medium-sized dendrite. *Scale bars* correspond to 1 μm.

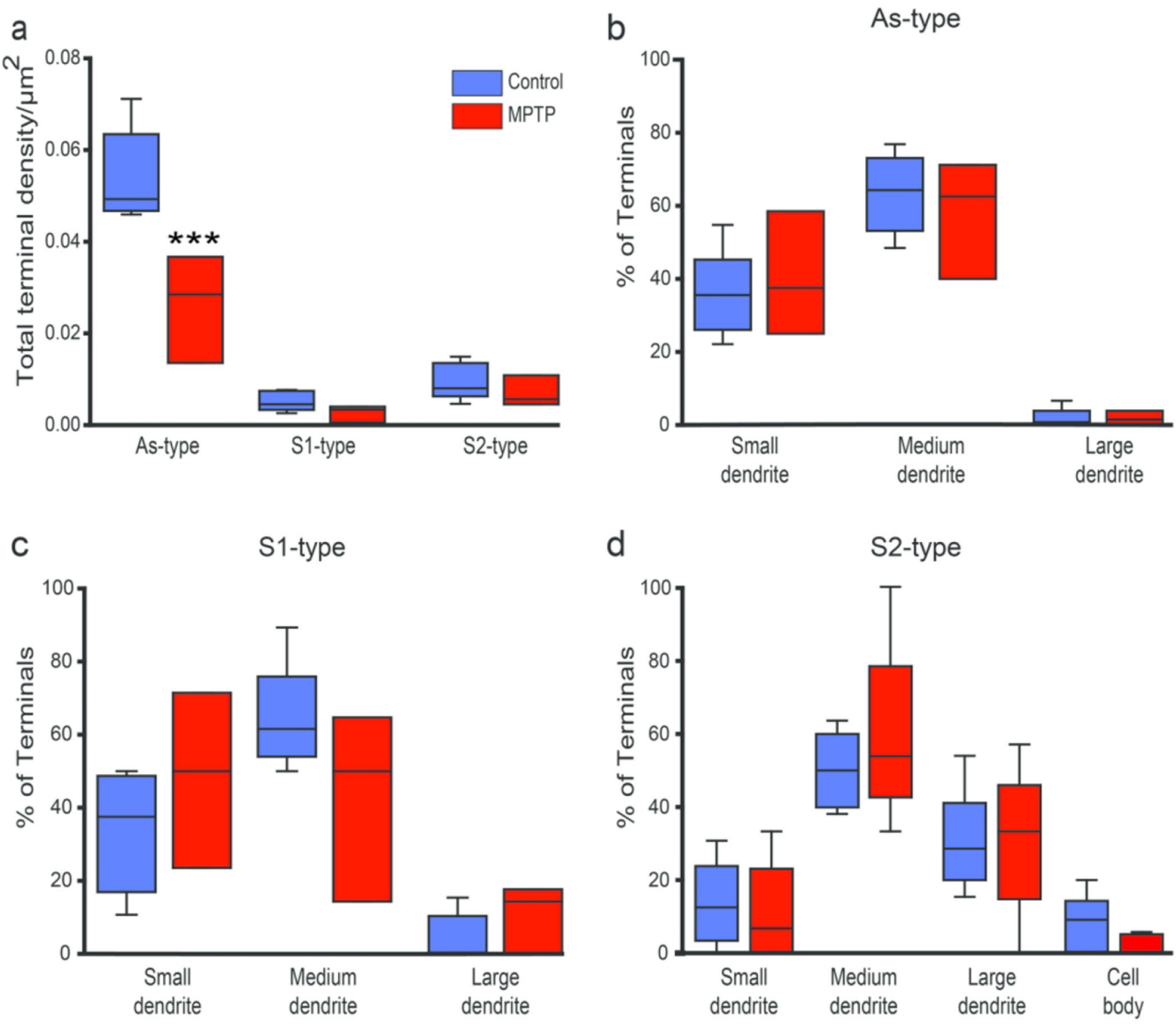

Fig. 4.

Relative prevalence and post-synaptic targets of GABAergic and glutamatergic terminals in the VApc. (**a**)Total density of each terminal sub-type in the VApc of control (N = 5) and parkinsonian (N = 3) monkeys, (**b-d**) Percentage of each terminal subtype in synaptic contact with dendritic profiles of different sizes in control (N = 5-6) and parkinsonian (N = 3-5) monkeys. Lines inside boxes indicate medians, top and bottom of boxes indicate 1st and 3rd quartile respectively, and whiskers indicate minimum and maximum data points. Significant decrease in As-type terminals between normal and MPTP-treated groups *** = $p<0.001$; S1-type terminals between control and MPTP group; $p=0.851$, S2-type terminals between control and MPTP group; $p= 0.941$, One-Way ANOVA (Holm-Sidak). Significant differences in the densities of As and S1 terminals in control: $p<0.001$ and MPTP: $p = 0.020$; significant differences in the densities of As and S2 terminals in control: $p<0.001$ and MPTP: $p = 0.004$; One Way ANOVA with Holm-Sidak post-hoc testing.

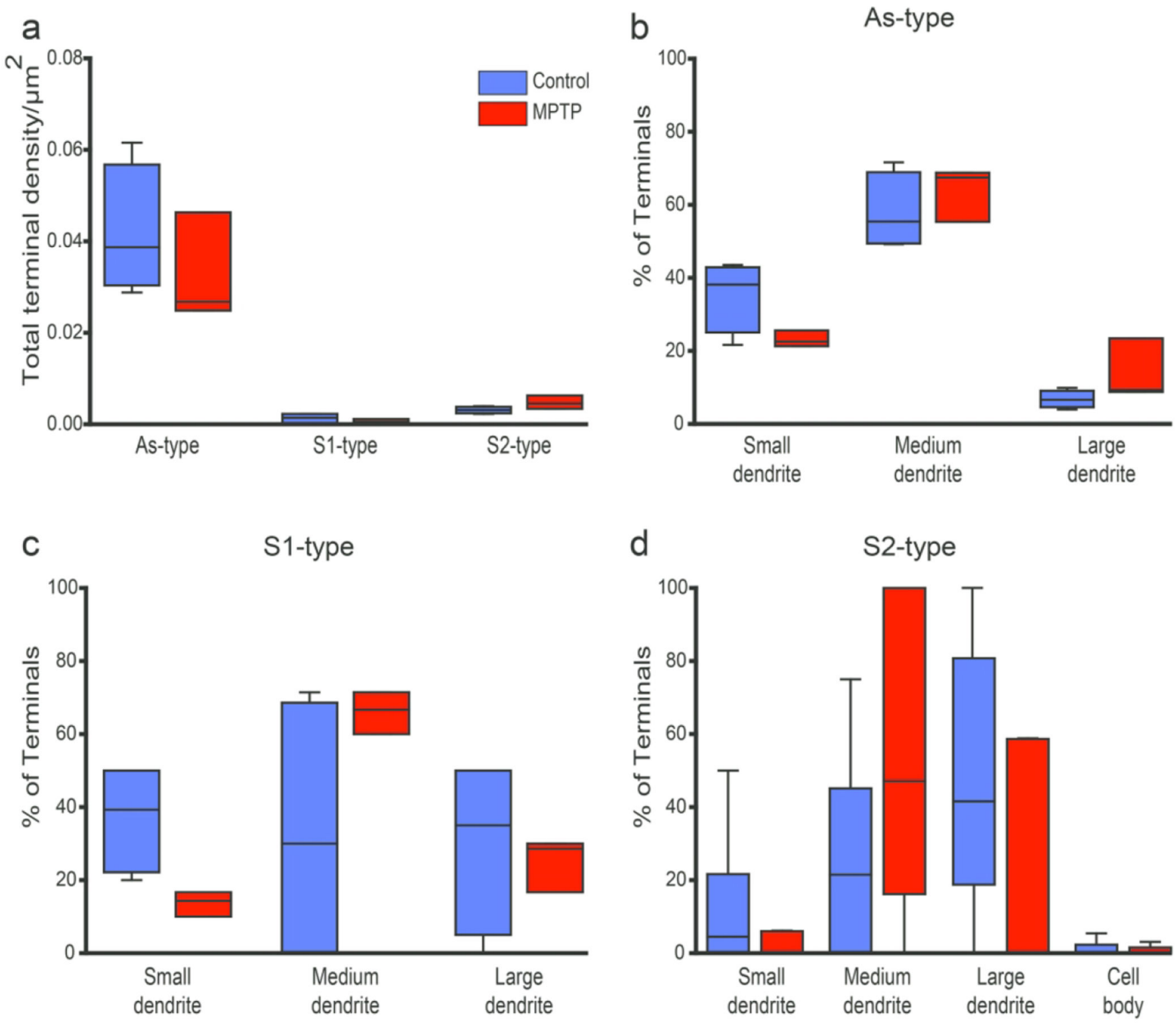

Fig. 5.

Relative prevalence and post-synaptic targets of GABAergic and glutamatergic terminals in the CM. (**a**) Total density of each terminal sub-type in the CM of control (N = 4) and parkinsonian (N=3) monkeys. (**b-d**) Percentage of each terminal subtype forming synaptic contact with dendritic profiles of different sizes in control (N=4-6) and parkinsonian (N=3-5) monkeys. Lines inside boxes indicate medians, top and bottom of boxes indicate 1st and 3rd quartile respectively, and whiskers indicate minimum and maximum data points. Significant difference in As-type terminals and S2-type terminals in control conditions $p=0.019 < 0.05$, Dunn's Method One Way Analysis of Variance on Ranks.

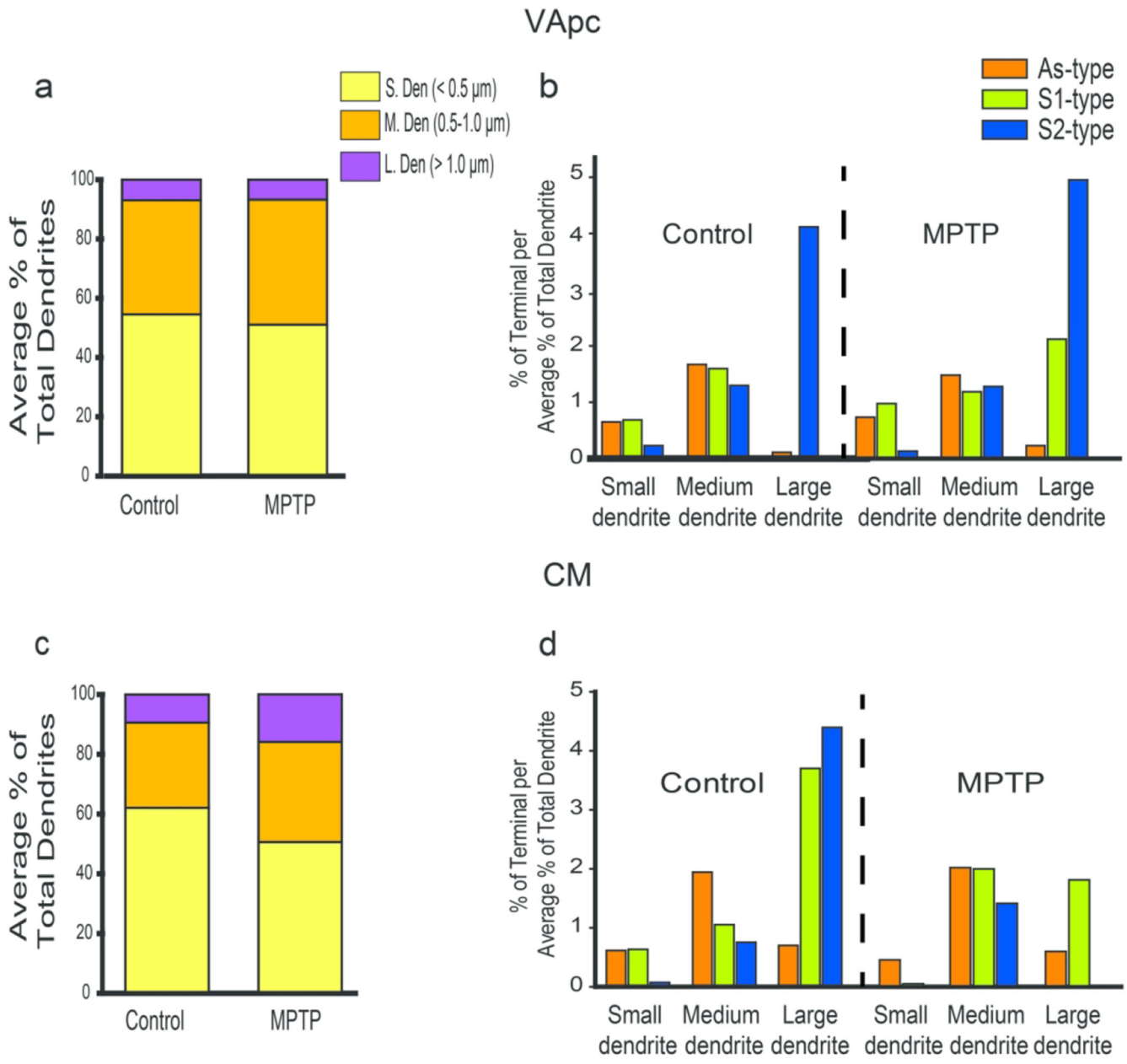

Fig. 6.

Preferential post-synaptic target of all terminal subtypes in the VApc and CM. (**a, c**) Average percentages of small, medium, and large dendrites in the VApc (**a**) and CM (**c**). (**b, d**) Ratio between the percent of terminal subtypes in contact with dendrites of different sizes and the relative proportion of small-, medium- or large-sized dendrites in the VApc (**b**) and CM (**d**) of control (N=4) and MPTP-treated (N=3) monkeys.

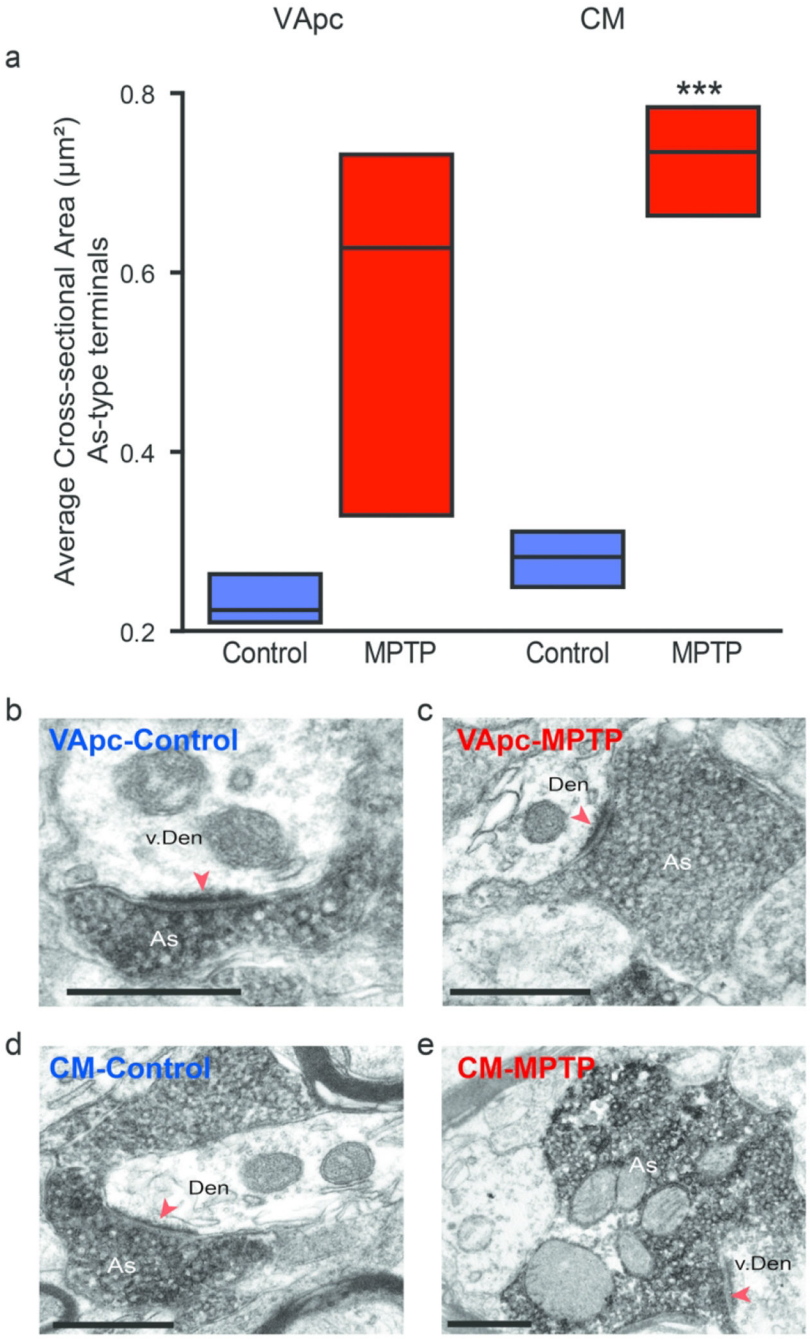

Fig. 7.

The cross sectional area of As-type terminals is enlarged in MPTP-treated monkeys. (**a**) vGluT1-positive terminals were analyzed in control (N=3) and parkinsonian (N=3) monkeys in the VApc (Control, n = 87 terminals; MPTP, n = 179 terminals), with an average area of 0.23 µm^2 in control and 0.56 µm^2 in MPTP-treated animals, and CM (Control, n = 94 terminals; MPTP-treated, n = 78 terminals), with an average area of 0.28 µm^2 in control and 0.73 µm^2 in MPTP-treated animals. Data are expressed as meant± SEM. (Statistical difference was found using a Student T-test in the CM, ***p<0.001). (**b-e**) Examples of

vGluT1-immunoreactive As-type terminals forming asymmetric axo-dendritic synapses in VApc or CM of control and parkinsonian monkeys. Scale bars: 500 nm.

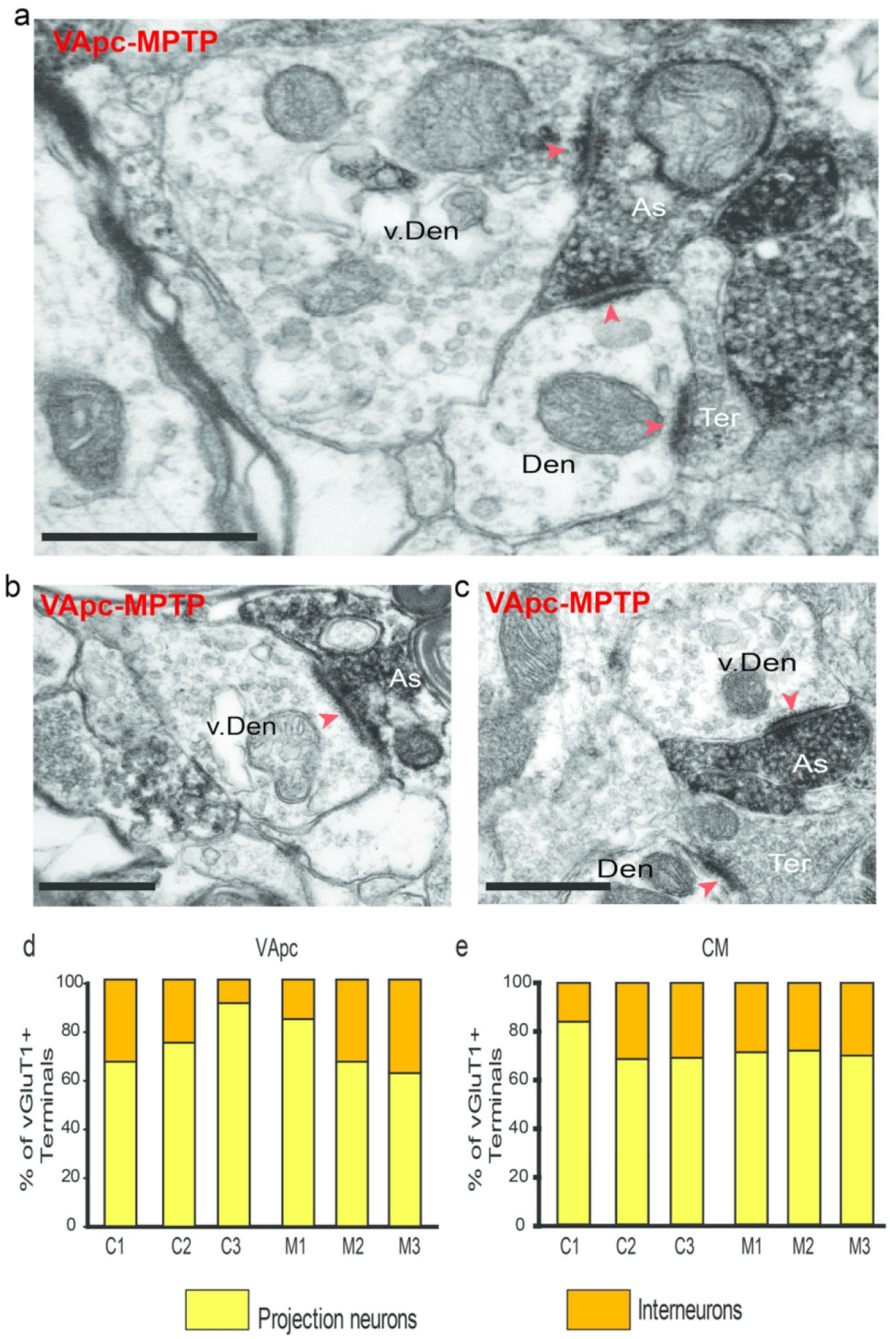

Fig.8.

vGluT1-labeled As-type (putative corticothalamic) terminals form synaptic contacts with vesicle-filled putative interneuron dendrites, (**a-c**) vGluT1-labeled terminal (As) making synaptic contact (red arrowheads) with a vesicle-filled interneuron's dendrite (v. Den) and a projection neuron (Den) in the VApc of a MPTP-treated monkey. An unlabeled bouton in asymmetric contact with the same dendrite is also shown (Ter), (**d-e**) Proportion of vGluT1-labeled terminals in the VApc (**d**) and the CM (**e**) in contact with dendrites of projection

neurons and interneurons in individual control (C1-C3) and parkinsonian (M1-M3) monkeys. *Scale bars* correspond to 500 nm.

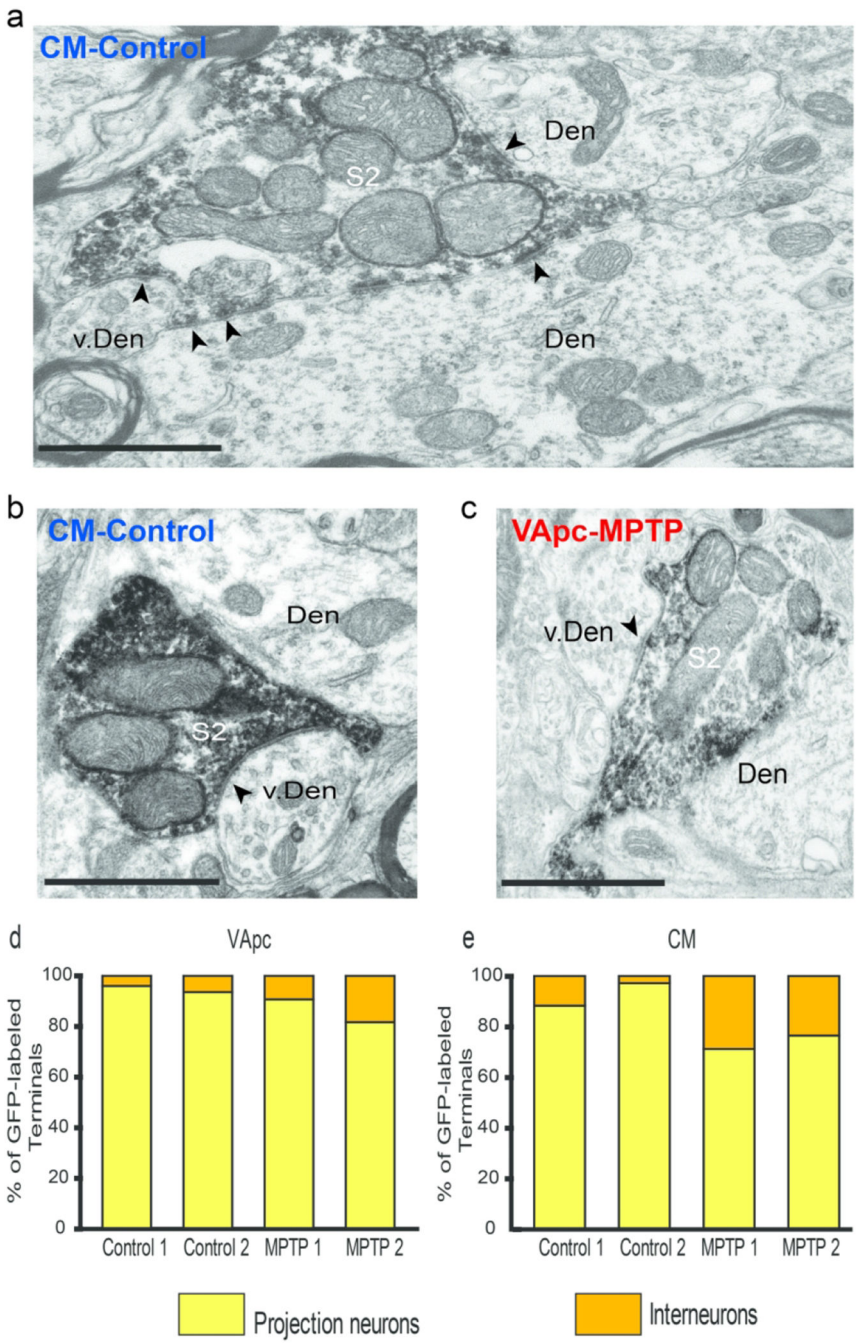

Fig. 9.

S2-type terminals form dual synaptic contacts with dendrites of projection neurons and vesicle-filled putative interneuron dendrites, (**a-c**) GFP-labeled terminal (S2) making synaptic contact (black arrowheads) with a vesicle-filled interneuron's dendrite (v. Den) and a projection neuron (Den) in CM (**a-b**) of a normal monkey and in the VApc (**c**) of a MPTP-treated monkey, (**d-e**) Proportion of GFP-labeled (pallidothalamic-S2) terminals in the VApc

(**d**) and the CM (**e**) in contact with dendrites of projection neurons or interneurons in control (N=2) and parkinsonian (N=2) monkeys. *Scale bars* correspond to 1μm.

Table 1

Animal Summary

Monkey #	Age at time of sacrifice	Sex	Control/ MPTP	Modified PRS score (based on (Wichmann et al., 2001))	Approximate delay between last dose of MPTP and sacrifice (years)	Cumulative dose of MPTP (mg/kg)
MR 165	3.5 years	Male	Control	----------	----------	----------
MR 249	3 years	Male	Control	----------	----------	----------
MR 252	3 years	Female	Control	----------	----------	----------
MR 186	3.5 years	Male	Control	----------	----------	----------
MR 194	4.75 years	Female	Control	----------	----------	----------
MR 271	3 years	Male	Control	----------	----------	----------
MR 209	14 years	Female	Control	----------	----------	----------
MR 231	9 years	Female	Control	----------	----------	----------
MR 232	13 years	Female	Control	----------	----------	----------
MR 255	3.9 years	Male	Control	----------	----------	----------
MR 259	2.6 years	Male	Control	----------	----------	----------
MR 272	3 years	Male	Control	----------	----------	----------
MR 244	17 years	Female	MPTP	12/30	11	17.5
MR 246	10 years	Female	MPTP	13.5/30	4	7.1
MR 245	14 years	Female	MPTP	10/30	8	4.15
MR 240	4 years	Male	MPTP	7/30	0.3	18.15
MR 269	5 years	Male	MPTP	16/30	1.6	8.2
MR 205	12 years	Female	MPTP	14/30	5	26.79
MR 247	15 years	Female	MPTP	14/30	2	9.5
MR 250	9 years	Male	MPTP	10/30	2	10.9
MR 218	4 years	Male	MPTP	5/30	1	2.8
MR 222	5 years	Male	MPTP	4.5/30	0.5	13.25

Table 2

Antibody information

Antigen	Immunizing species	Vendor (Primary)	Antibodies dilution used	Secondary antibodies dilution used	Vendor (Secondary)	Purpose	RRID
vesicular GABA Transporter (vGAT)	Mouse	R&D Systems, Minneapolis, MN catalog no. MAB6847	1:5,000	Horse anti Mouse 1:200 (biotinylated)	Vector, Burlingame, CA catalog no. BA2000	To identify GABAergic terminals	AB_2814814
Glutamic Acid Decarboxylase 67 (GAD67)	Mouse	Millipore, Burlington, MA catalog no. MAB5406	1:5,000	Horse anti Mouse 1:200 (biotinylated)	Vector, Burlingame, CA catalog no. BA2000	To identify GABAergic terminals	AB_2278725
Calbindin D28k (Cb)	Goat	R&D Systems, Minneapolis, MN catalog no. AF3320	1:1,000	Horse ant Goat 1:200 (biotinylated)	Vector, catalog no. BA9500	To delineate thalamic nuclei	AB_2254256
GFP	Rabbit	Life Tech, Waltham, MA catalog no. A11122	1:5,000	Goat anti Rabbit 1:200 (biotinylated)	Vector, Burlingame, CA catalog no. BA9400	To identify EYFP-positive elements (EYFP is a variant of GFP)	AB_221569
vesicular Glutamate Transporter 1 (vGluT1)	Guinea Pig	Millipore, Burlington, MA catalog no. AB5905	1:5,000	Goat anti Guinea Pig 1:200 (biotinylated)	Vector, Burlingame, CA catalog no. BA7000	To identify corticothalamic (i.e. As) terminals	AB_2814813
GABA	Rabbit	Sigma, St. Louis, MO catalog no. A2052	1:1,000	Goat anti Rabbit 1:50 (gold; 15nm gold particle)	BBI, Madison, WI catalog no. EMAR-15	To identify GABAergic terminals	AB_477652
Tyrosine hydroxylase (TH)	Mouse	Millipore, Burlington, MA catalog no. MAB318	1:1,000	Horse anti Mouse 1:200 (biotinylated)	Vector, Burlingame, CA catalog no. BA2000	To identify dopamine-containing neurons and terminals	AB_2201528